Electronic Supplementary Information
for:

# The characterisation of commercial 2D carbons: graphene, graphene oxide and reduced graphene oxide.

Peter W. Albers,[a] Valeri Leich,[b] Anibal J. Ramirez-Cuesta,[c] Yongqiang Cheng,[c] Jonas Hönig,[d] Stewart F. Parker[e,f]*

[a]Evonik Technology & Infrastructure GmbH, 915 D115, Rodenbacher Chaussee 4. 63457 Hanau-Wolfgang, Germany
[b]Evonik Operations GmbH - Creavis, Paul-Baumann-Straße 1, 45772 Marl, Germany
[c]Neutron Scattering Division, Oak Ridge National Laboratory, Oak Ridge Tennessee 37831, United States
[d]Evonik Operations GmbH, Kirschenallee, 64293 Darmstadt, Germany
[e]ISIS Pulsed Neutron and Muon Source, STFC Rutherford Appleton Laboratory, Chilton, OX11 0QX, UK
[f]School of Chemistry, Joseph Black Building, University of Glasgow, Glasgow, G12 8QQ, UK

*Corresponding author. Email: stewart.parker@stfc.ac.uk

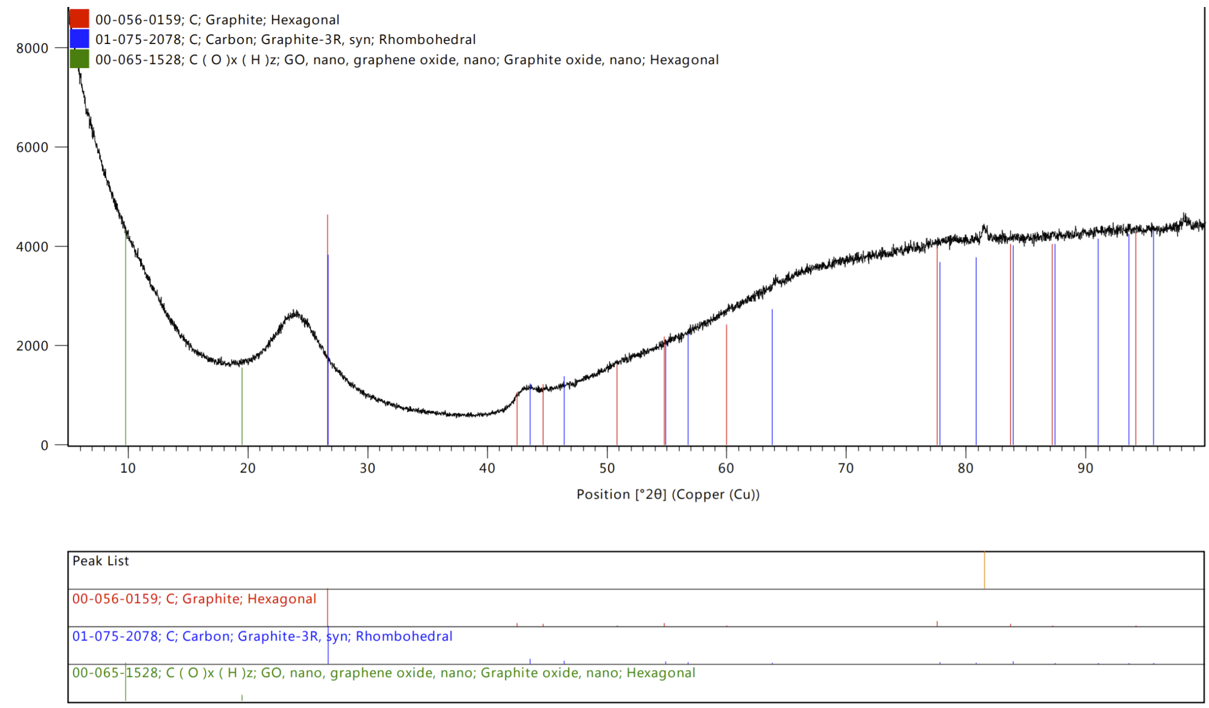


**Fig. S1**. XRD fit for 1_GO

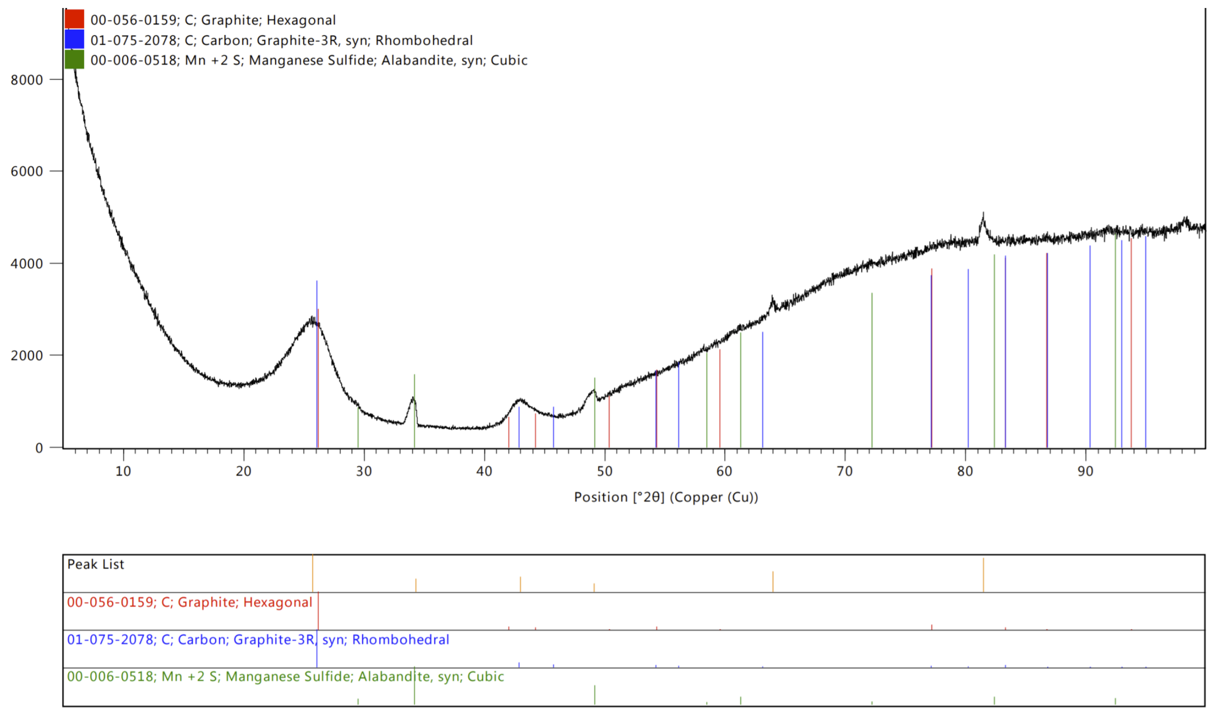


**Fig. S2**. XRD fit for 2_rGO

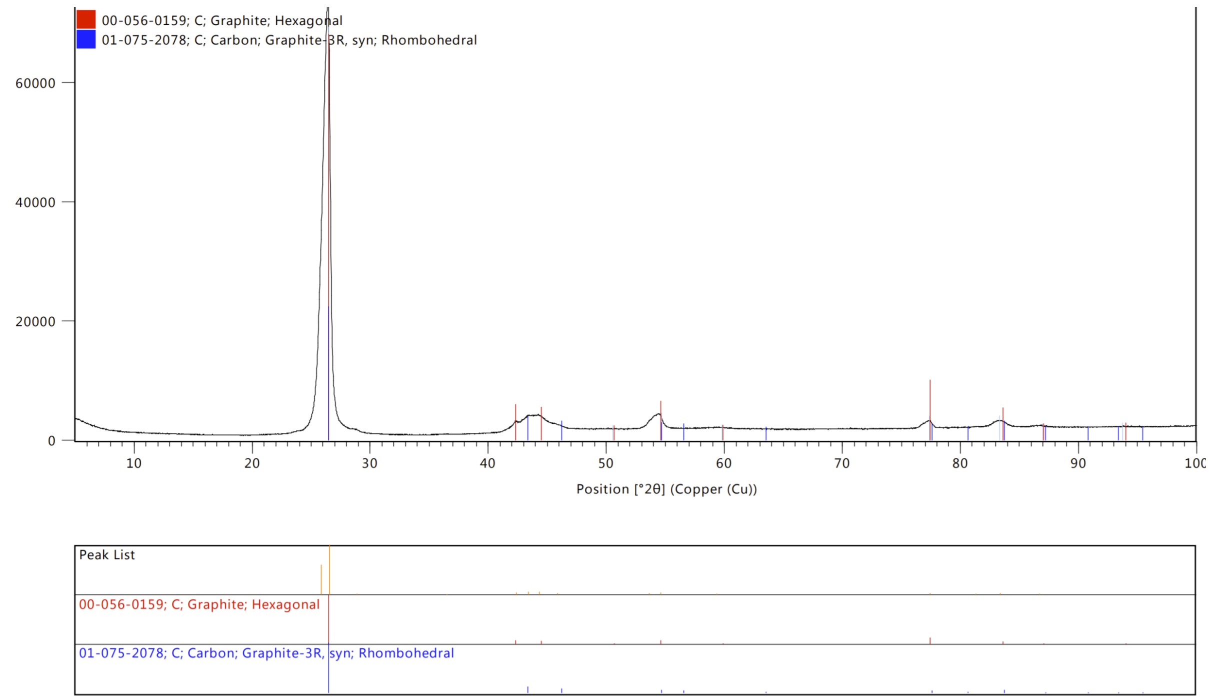


**Fig. S3**. XRD fit for 3_GNP

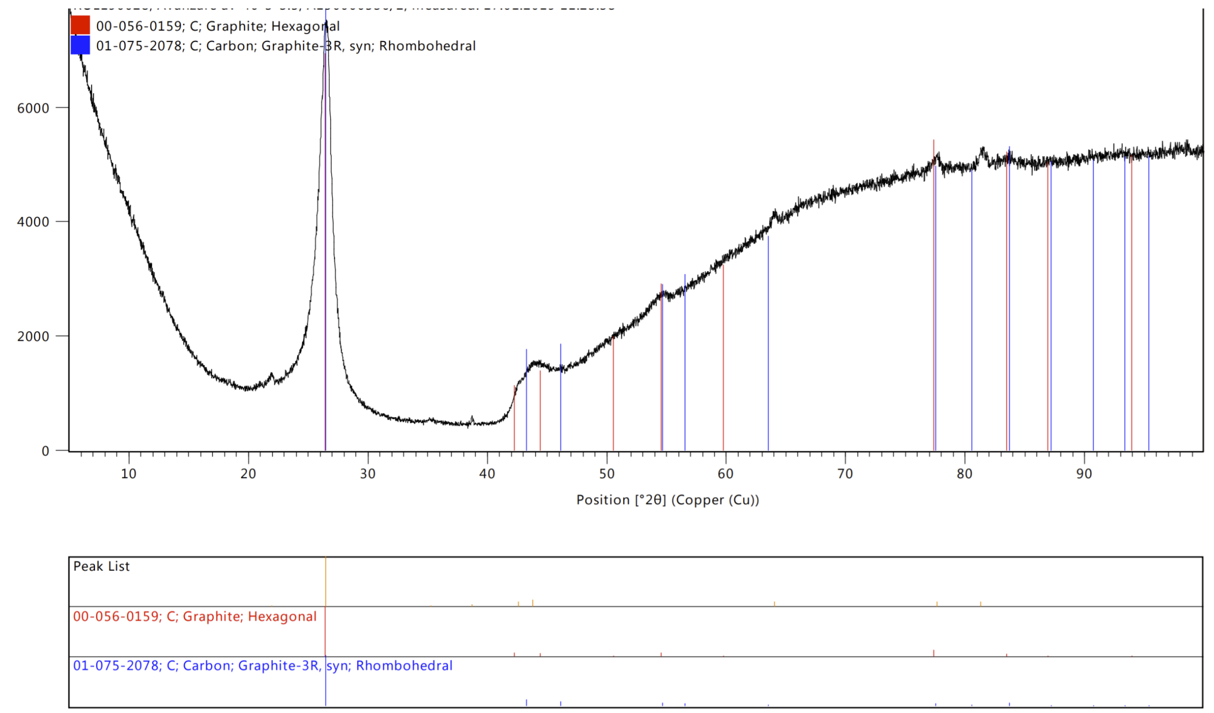


**Fig. S4**. XRD fit for 4_rGO

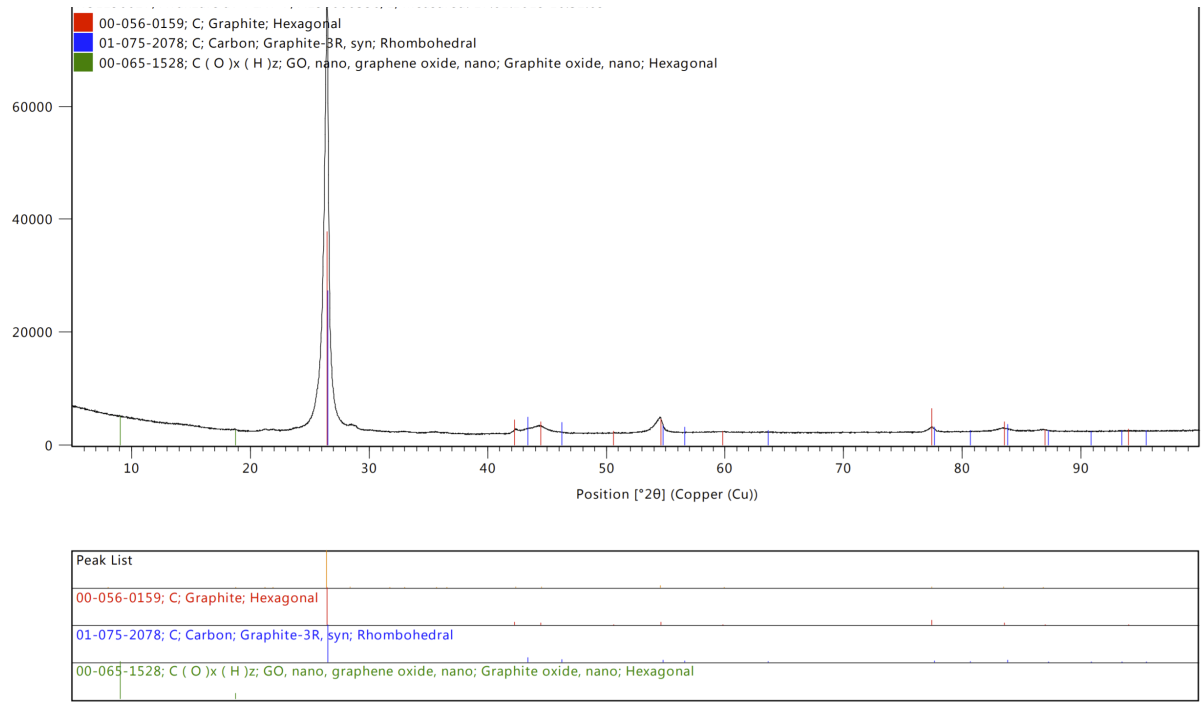


**Fig. S5**. XRD fit for 5_GNP

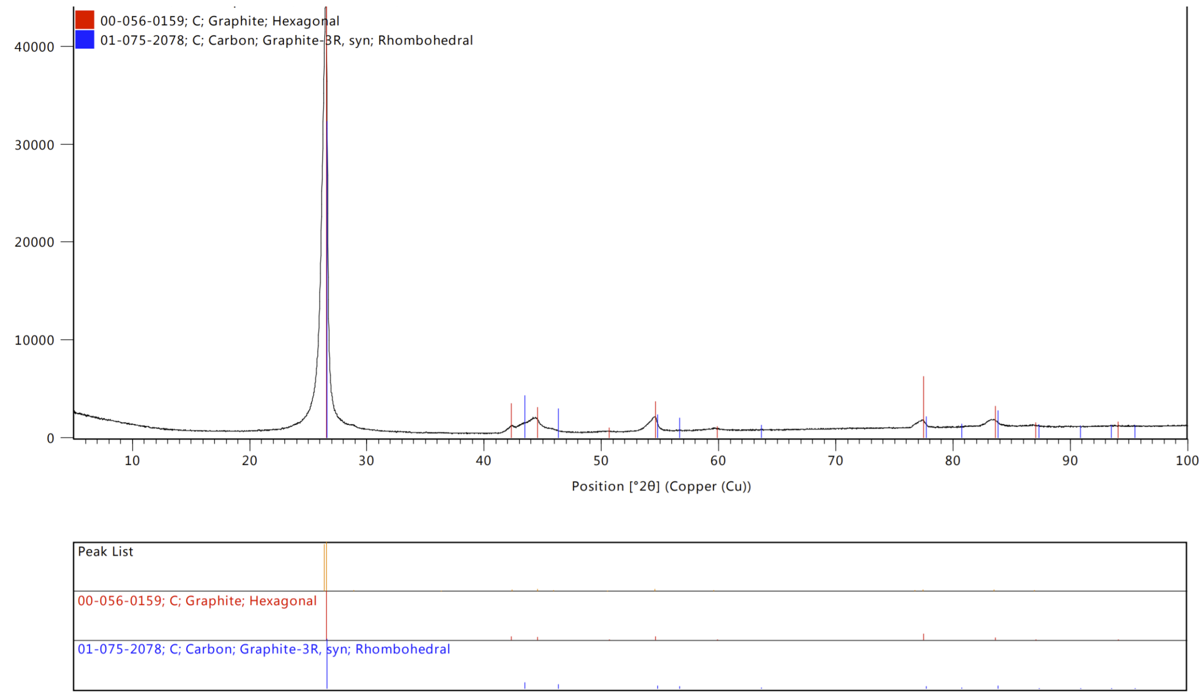


**Fig. S6**. XRD fit for 6_GNP

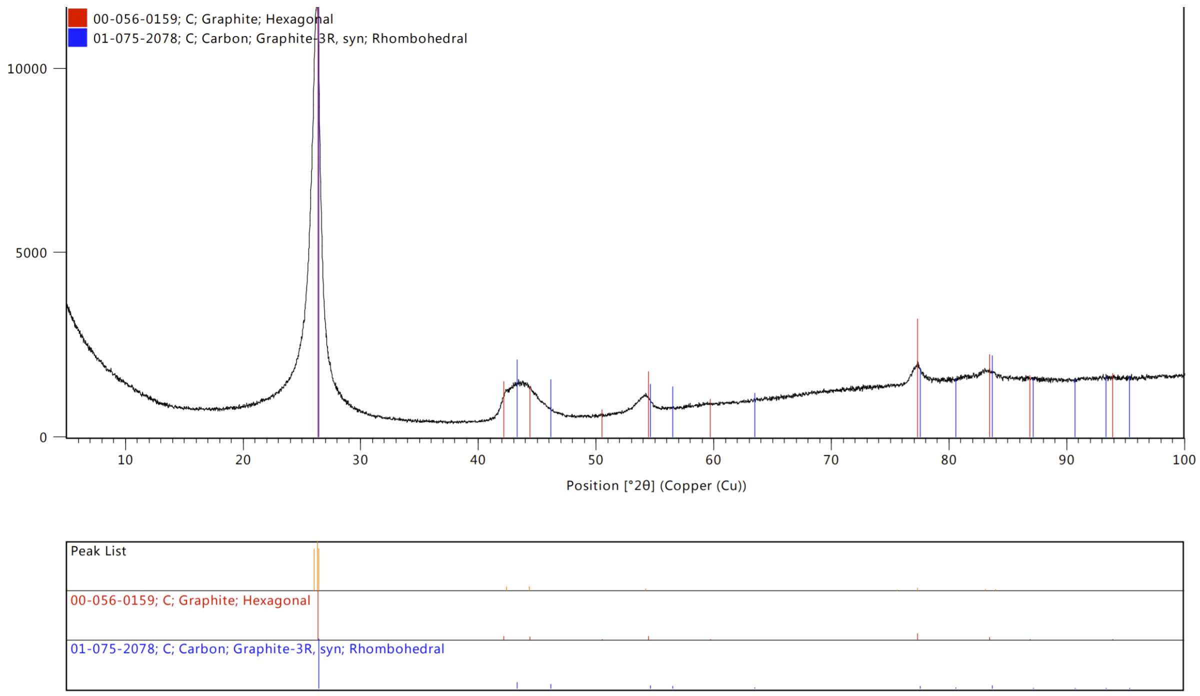


**Fig. S7**. XRD fit for 7_GO

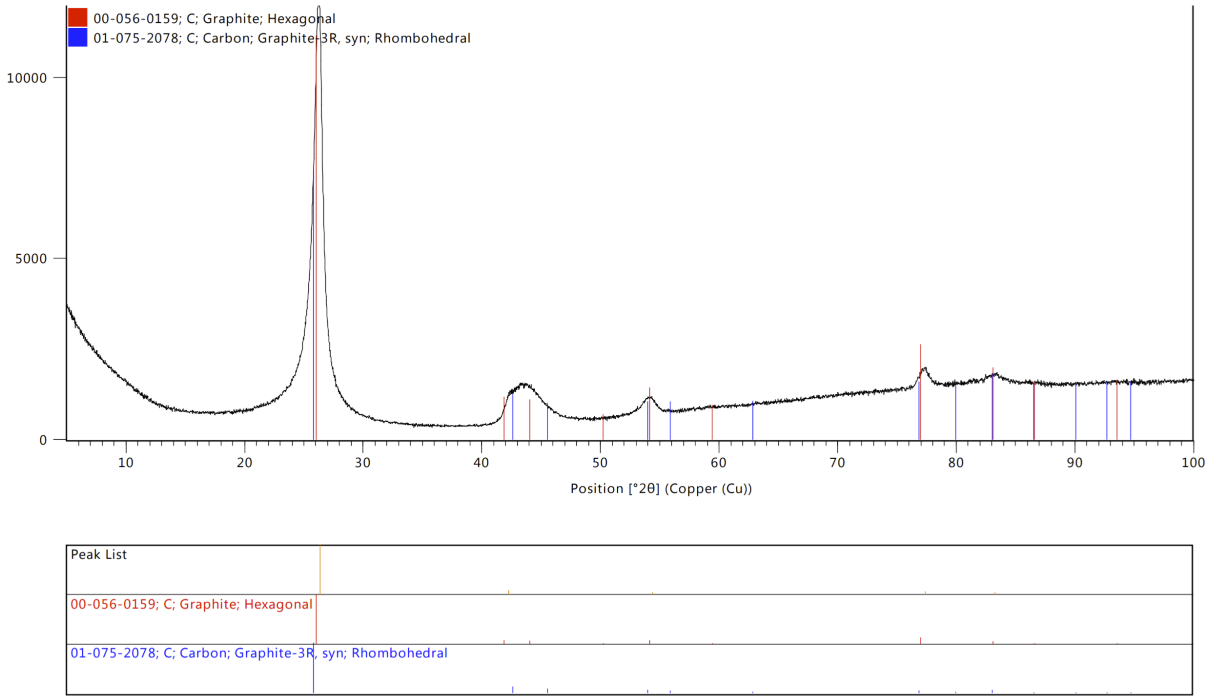


**Fig. S8**. XRD fit for 8_rGO

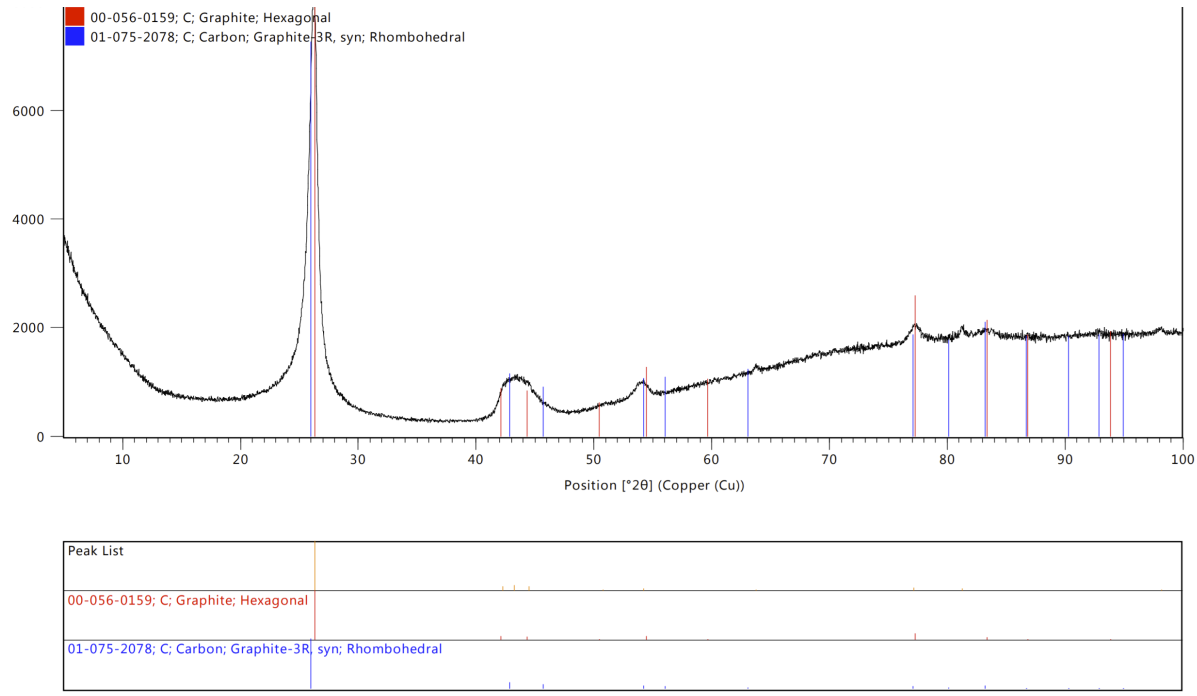


**Fig. S9**. XRD fit for 9_GNP

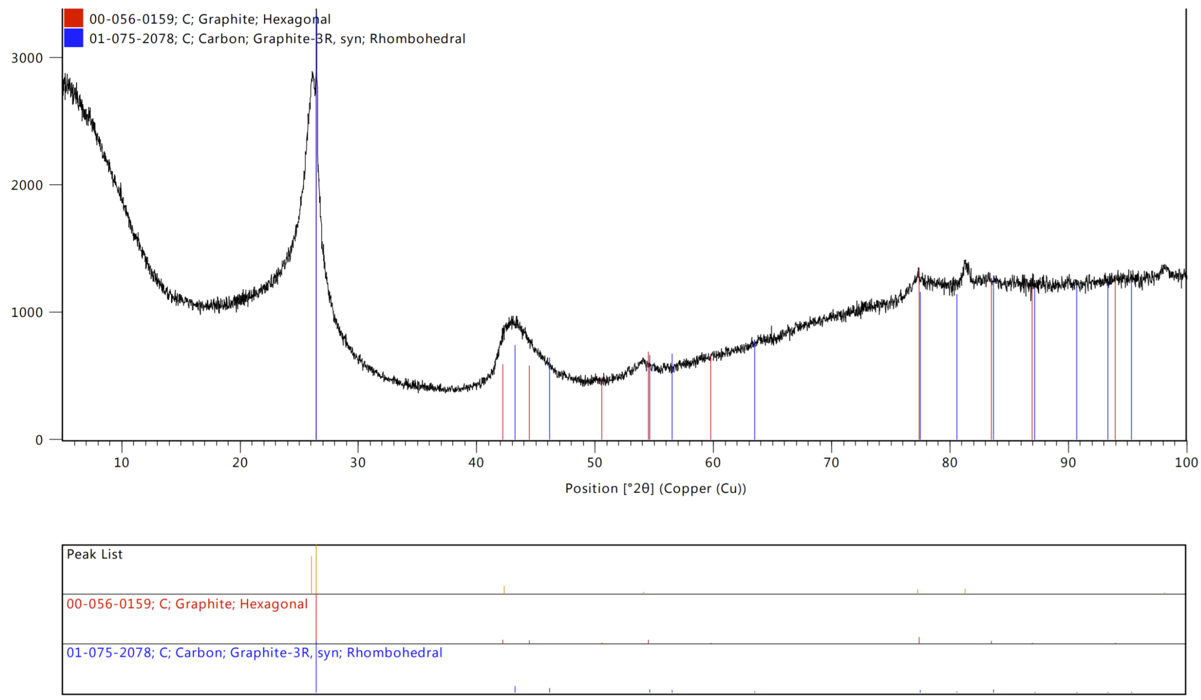


**Fig. S10**. XRD fit for 10_GO

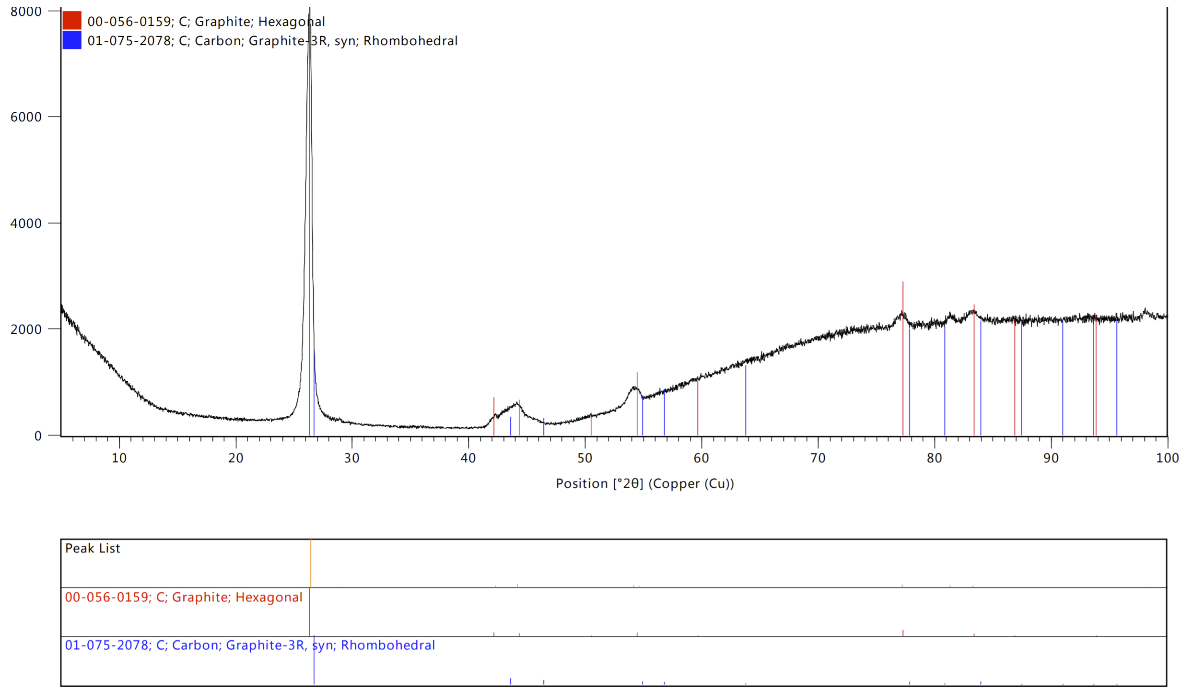


**Fig. S11**. XRD fit for 11_GNP

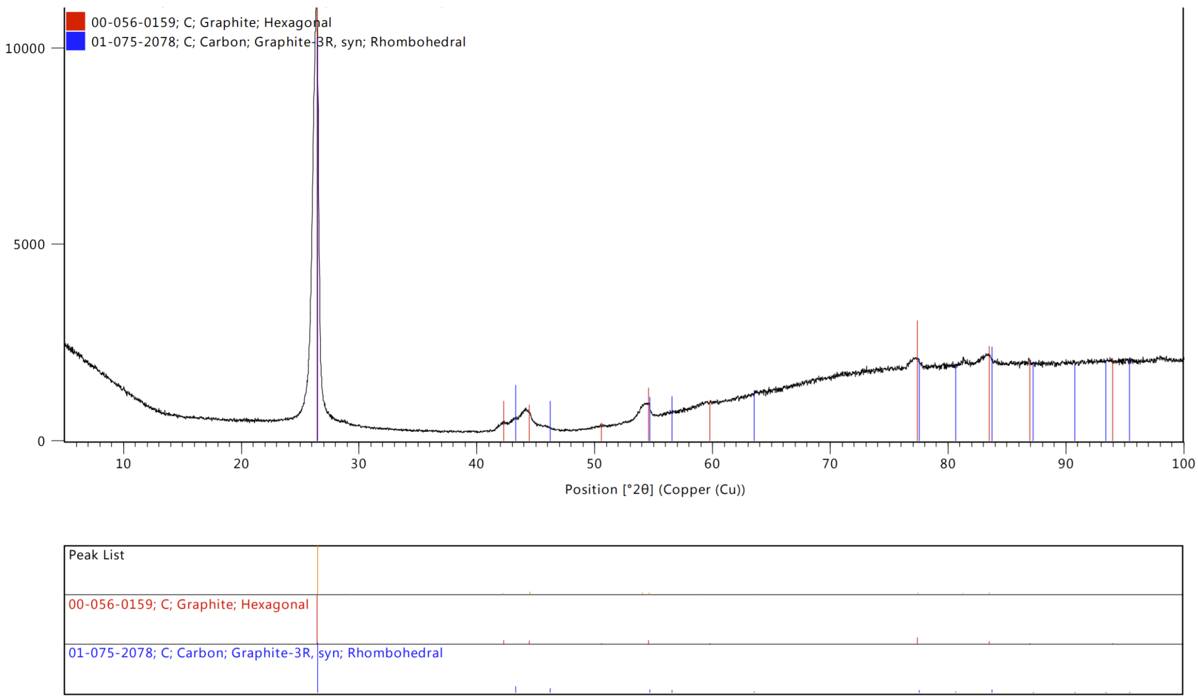


**Fig. S12**. XRD fit for 12_GNP

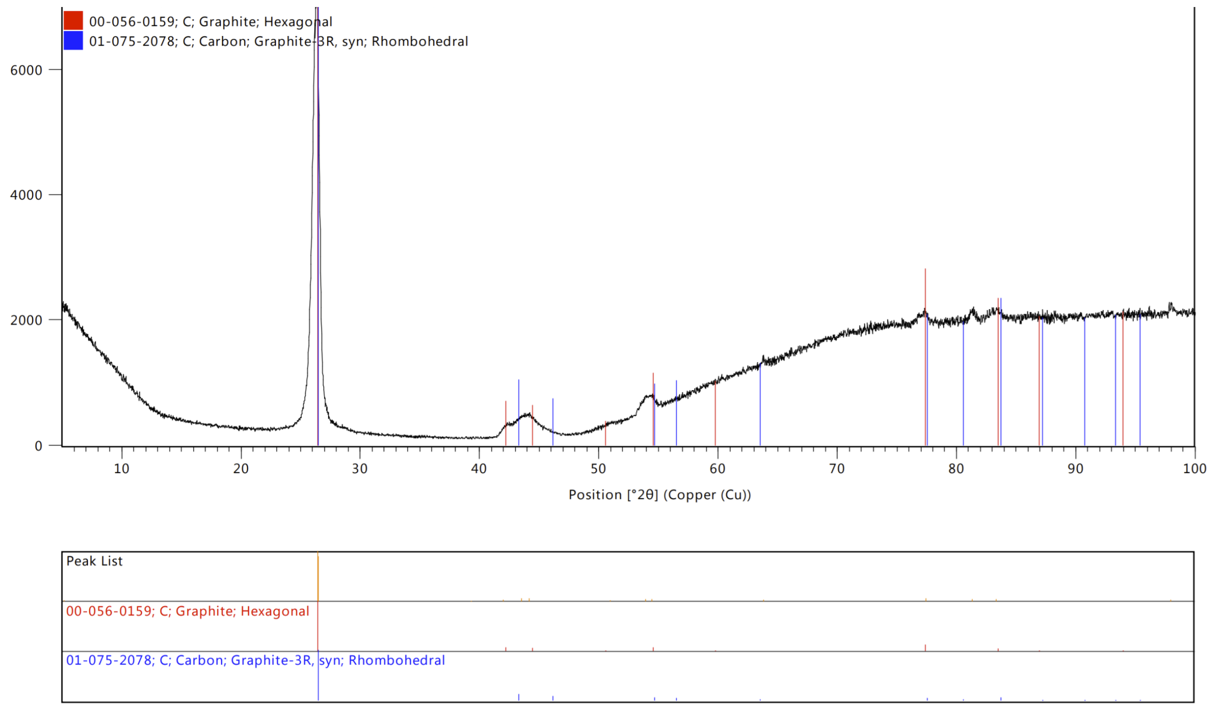


**Fig. S13**. XRD fit for 13_GNP

3_GNP

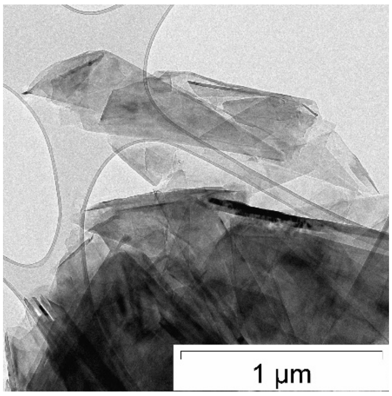


9_GNP

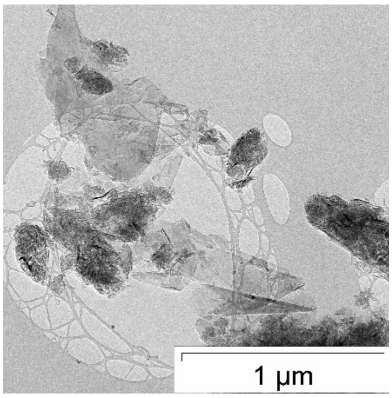


13_GNP

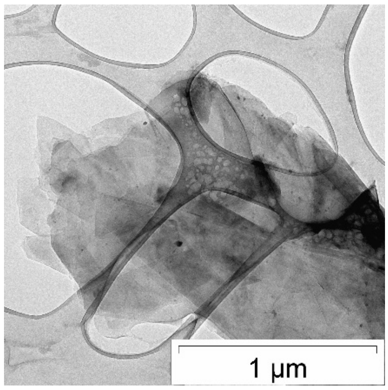


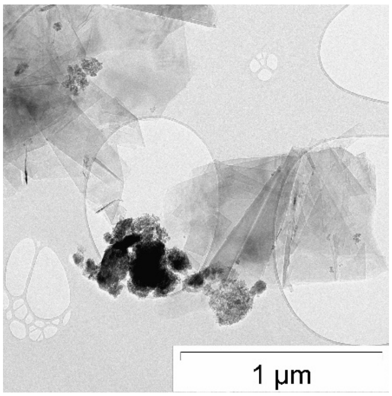


11_GNP

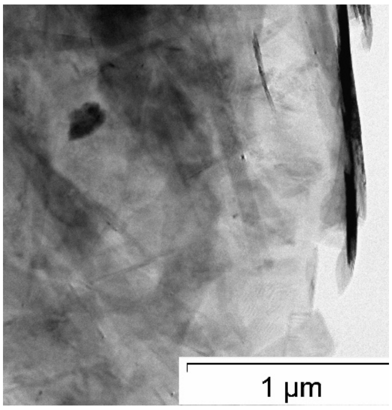


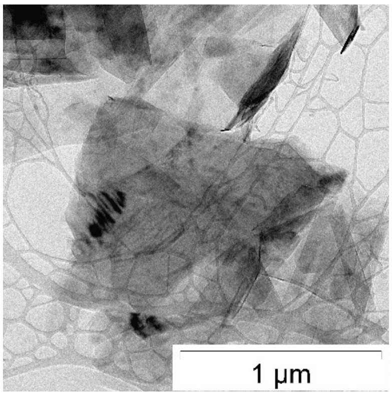


12_GNP

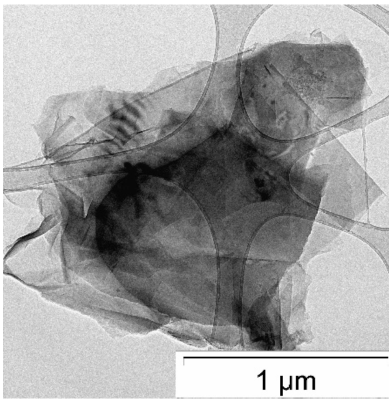

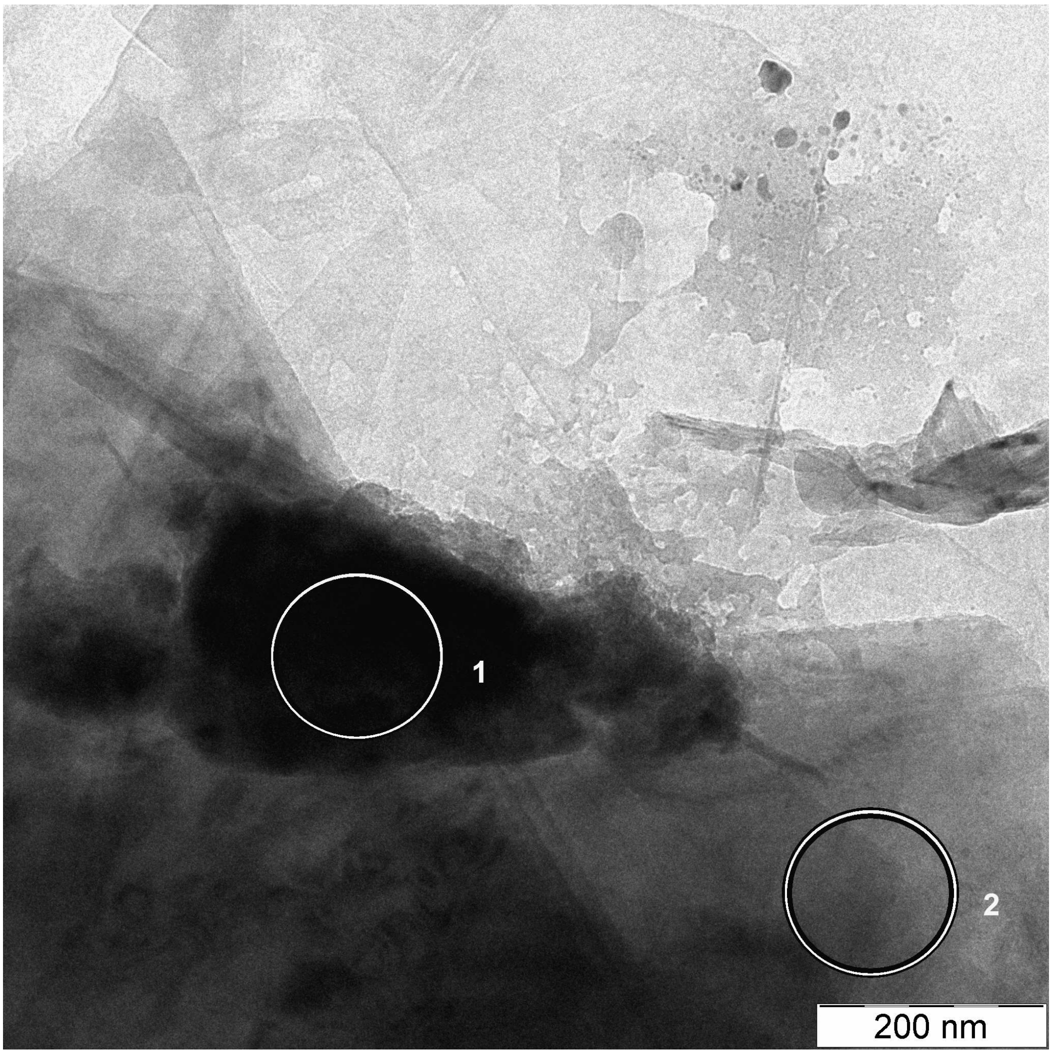


**Fig. S15.** 200 keV TEM image of a 2D carbon.

**Table S1**
EDX spot analyses in the TEM Jeol 2010F areas analysed marked by circles in Fig. S2.

| | Area 1 | | Area 2 | |
|---|---|---|---|---|
| Element | Wt.% | At.% | Wt.% | At.% |
| C | 62.18 | 79.23 | 88.75 | 92.90 |
| O | 10.83 | 10.36 | 6.83 | 5.36 |
| Na | 0.86 | 0.57 | 0.33 | 0.18 |
| Mg | 0.38 | 0.24 | | |
| Al | 1.72 | 0.98 | | |
| Si | 5.56 | 3.03 | 0.14 | 0.06 |
| S | 0.50 | 0.24 | 3.11 | 1.22 |
| Cl | 0.46 | 0.20 | 0.48 | 0.17 |
| K | 0.32 | 0.12 | 0.14 | 0.04 |
| Ca | 2.83 | 1.08 | | |
| Cr | 1.63 | 0.48 | | |
| Mn | 0.27 | 0.08 | | |
| Fe | 11.13 | 3.05 | 0.21 | 0.05 |
| Ni | 1.33 | 0.35 | | |

**A**

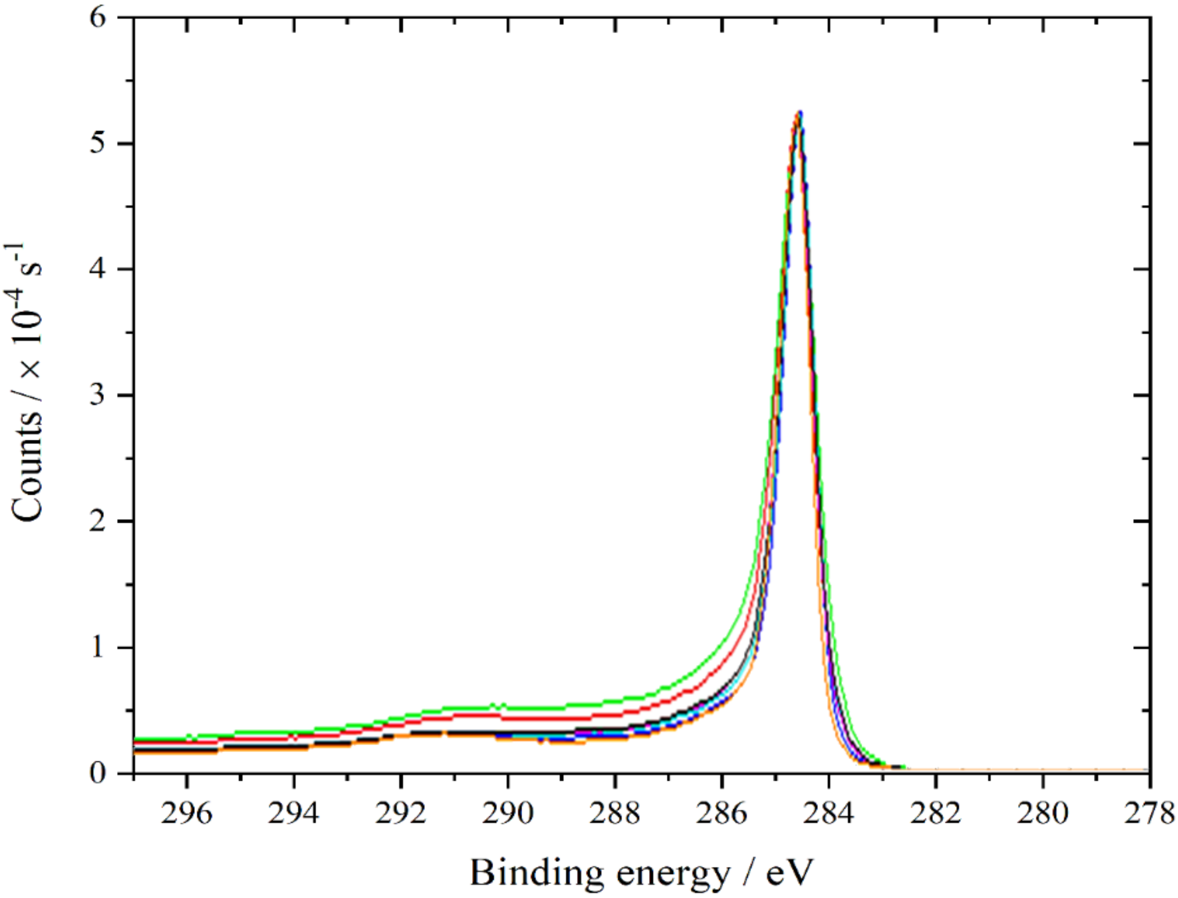

Counts / × $10^{-4}$ $s^{-1}$
0
1
2
3
4
5
6
296
294
292
290
288
286
284
282
280
278
Binding energy / eV


**B**

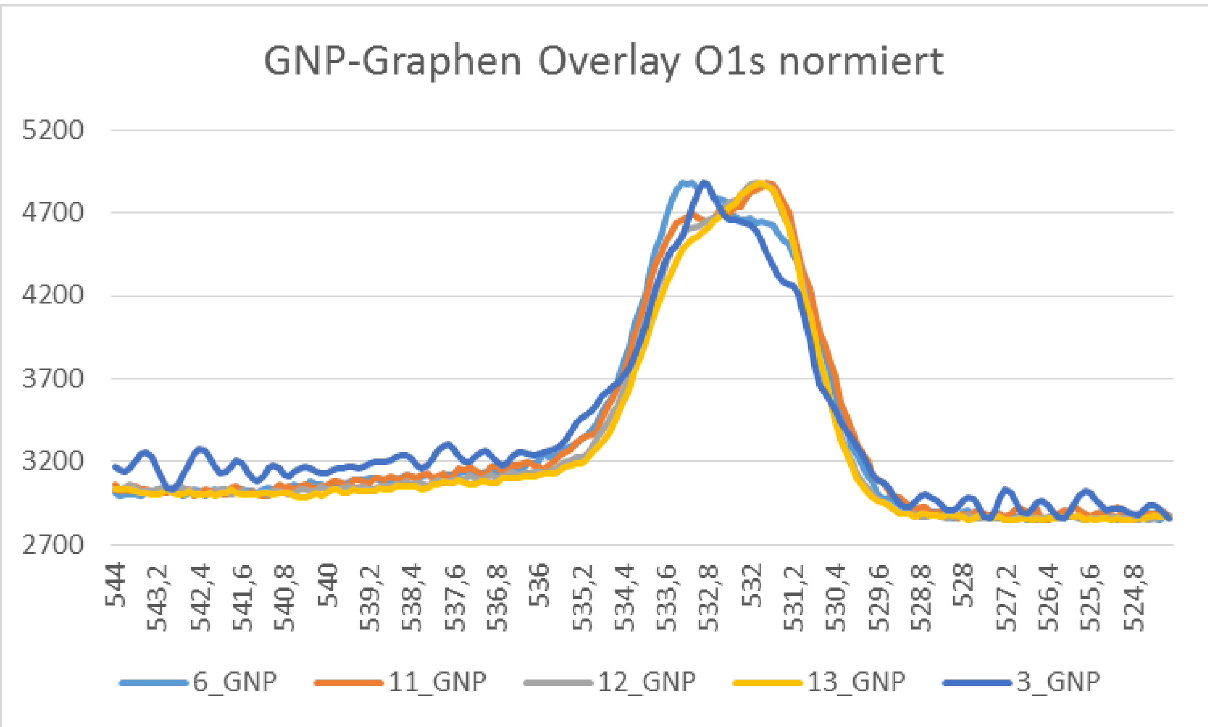

GNP-Graphen Overlay O1s normiert
5200
4700
4200
3700
3200
2700
544
543,2
542,4
541,6
540,8
540
539,2
538,4
537,6
536,8
536
535,2
534,4
533,6
532,8
532
531,2
530,4
529,6
528,8
528
527,2
526,4
525,6
524,8
6_GNP
11_GNP
12_GNP
13_GNP
3_GNP

C

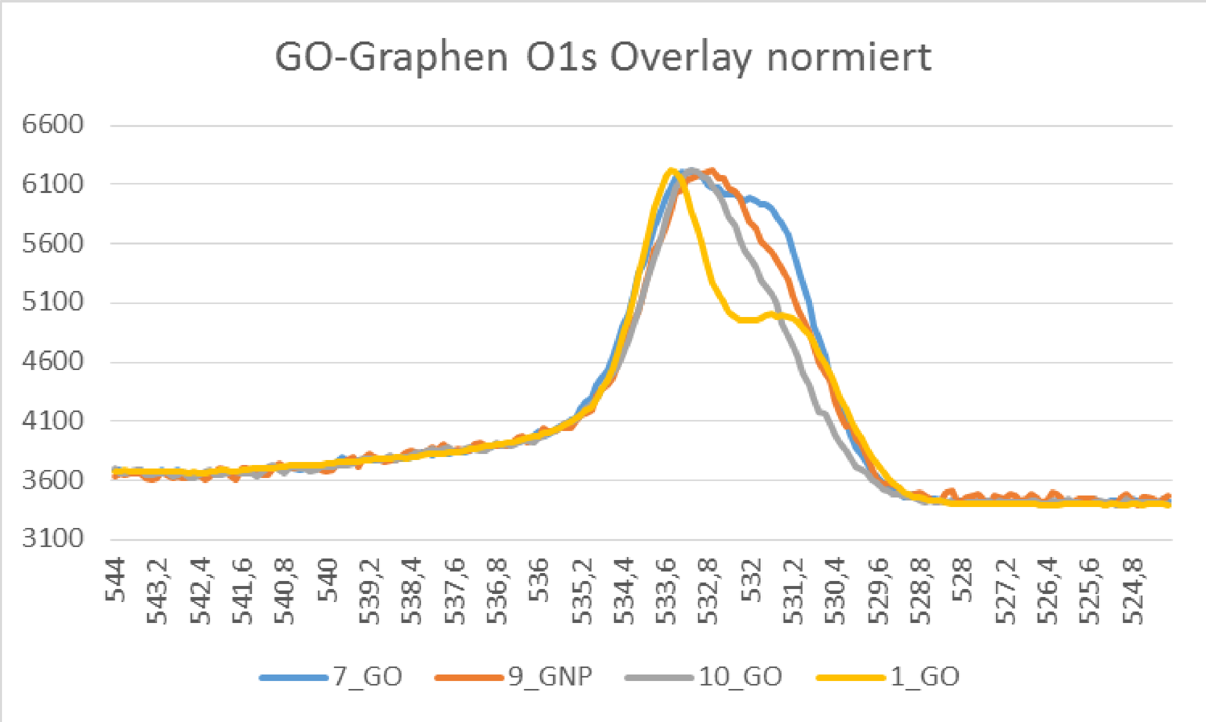


D

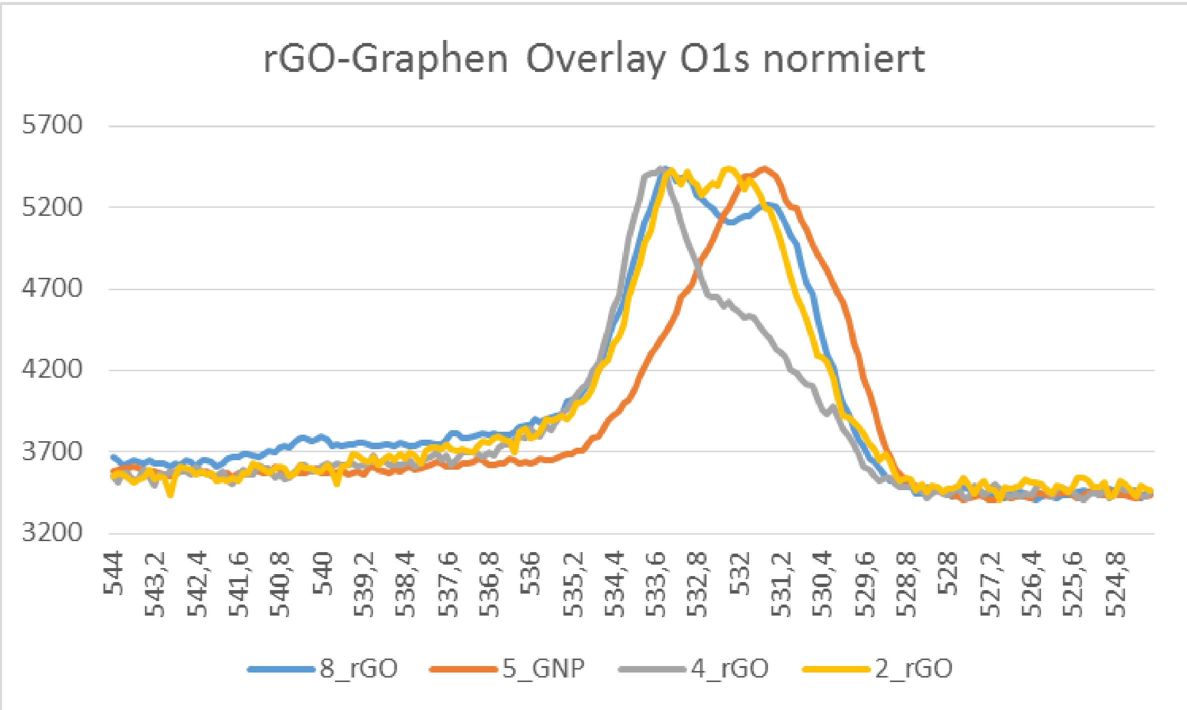


**Fig. S16.** A: Representative O1s XPS spectra of the GNP samples. B-D: Normalised to the largest peak, O1s XPS spectra of the 2D carbon samples.

**Table S2**
Previous data [1] on 3D carbons, spherical aggregates/agglomerates of commercial carbon blacks before and after oxidizing aftertreatment. In a separate oxidation experiment on gb original, after moderate post-oxidation with $O_3$, XPS revealed an increase in surface-oxygen from 1.45 to 13.5%.

| Carbon black, oxidation treatment[a] | H / wt.% | BET / $m^2$ $g^{-1}$ | XPS O / at.% | XPS O1s C–OH/C=O |
|---|---|---|---|---|
| ac original | 0.018 | 40 | 0.04 | ? |
| lb original | 0.265 | 20 | 0.3 | 2.2 |
| fb original | 0.33 | 120 | 0.7 | 6.6 |
| fb $HNO_3$ | 0.26 | ca. 140 | 9.8 | 2.2 |
| gb original | 0.37 | 360 | 1.45 | 1.4 |
| gb $NO_2$ | 0.35 | ca. 460 | 8.5 | 2.7 |
| gb $NO_2$ | 0.38 | " | 9.1 | 2.2 |
| gb $NO_2$ | 0.44 | " | 11.8 | 2.2 |
| gb $HNO_3$ | 0.32 | " | 10.5 | 4.3 |
| gb $O_3$ | 0.53 | " | 19.3 | 1.6 |

[a]fb: furnace black, gb: gas black, lb: lamp black (all Degussa-Hüls), ac: acetylene black (Denka Black).

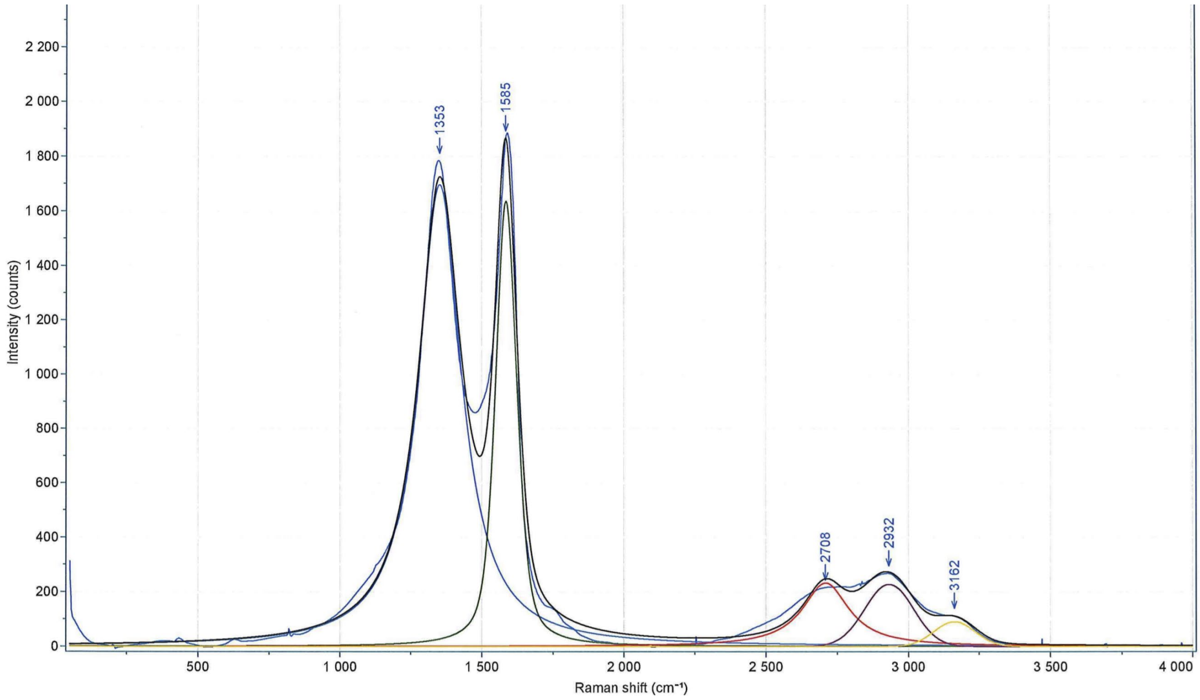


**Fig. S17**. Raman spectrum for 1_GO

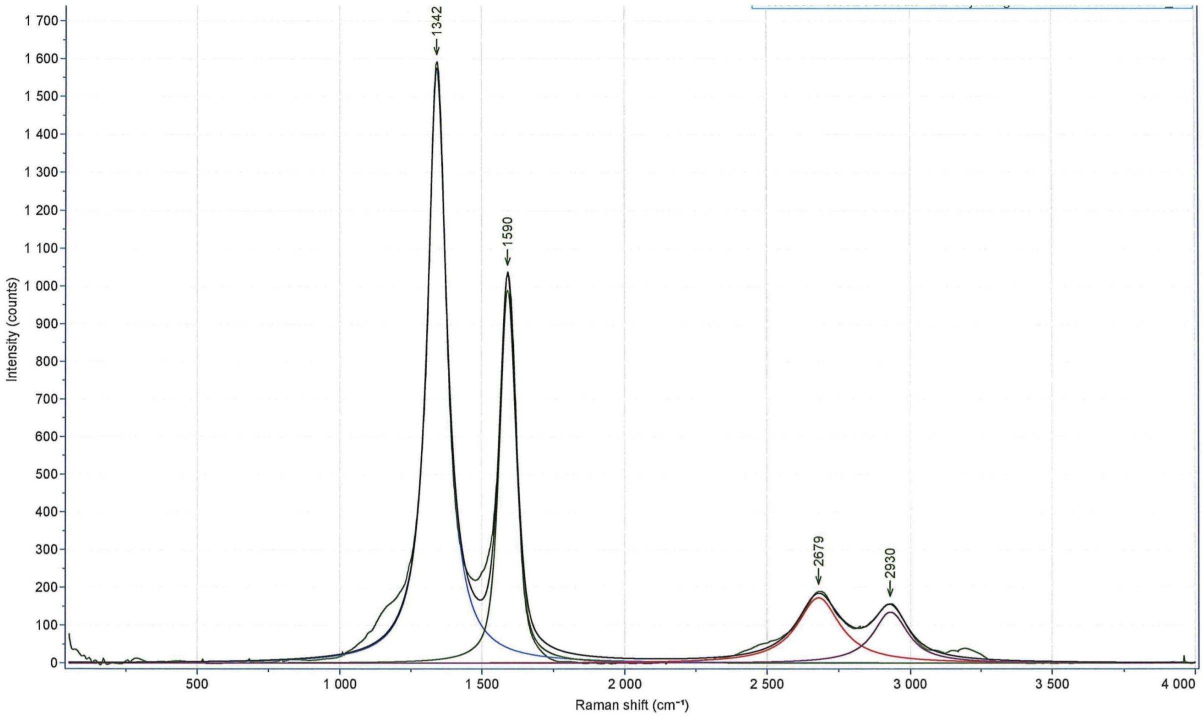


**Fig. S18**. Raman spectrum for 2_rGO

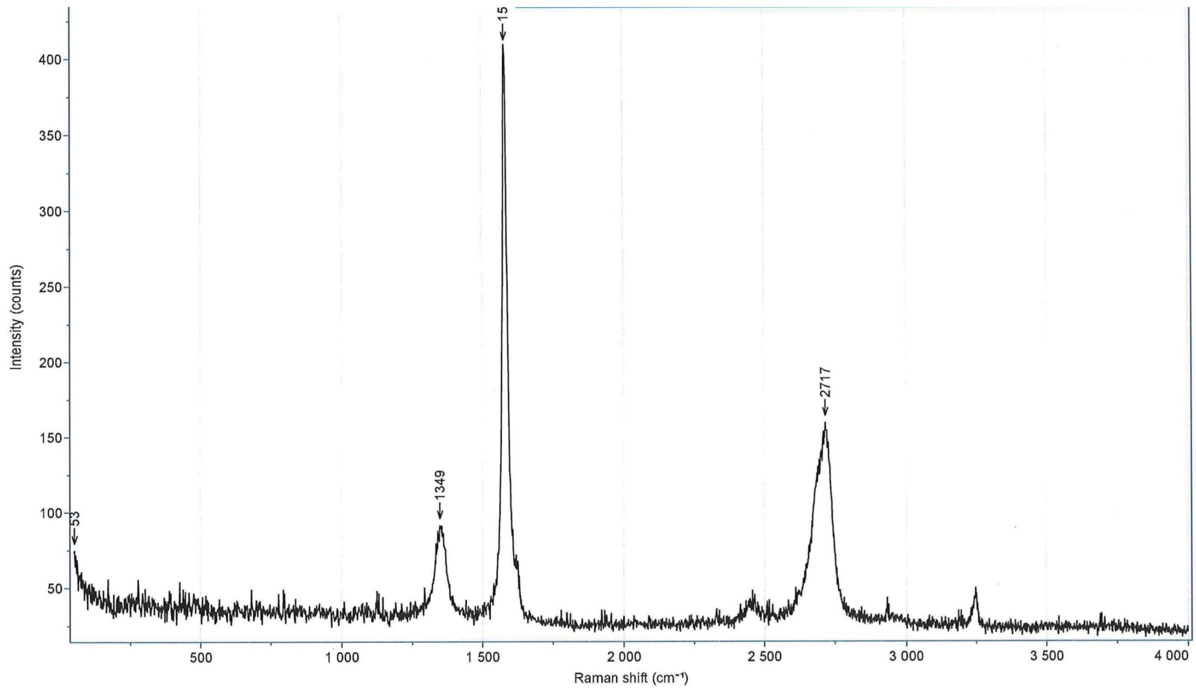


**Fig. S19**. Raman spectrum for 3_GNP

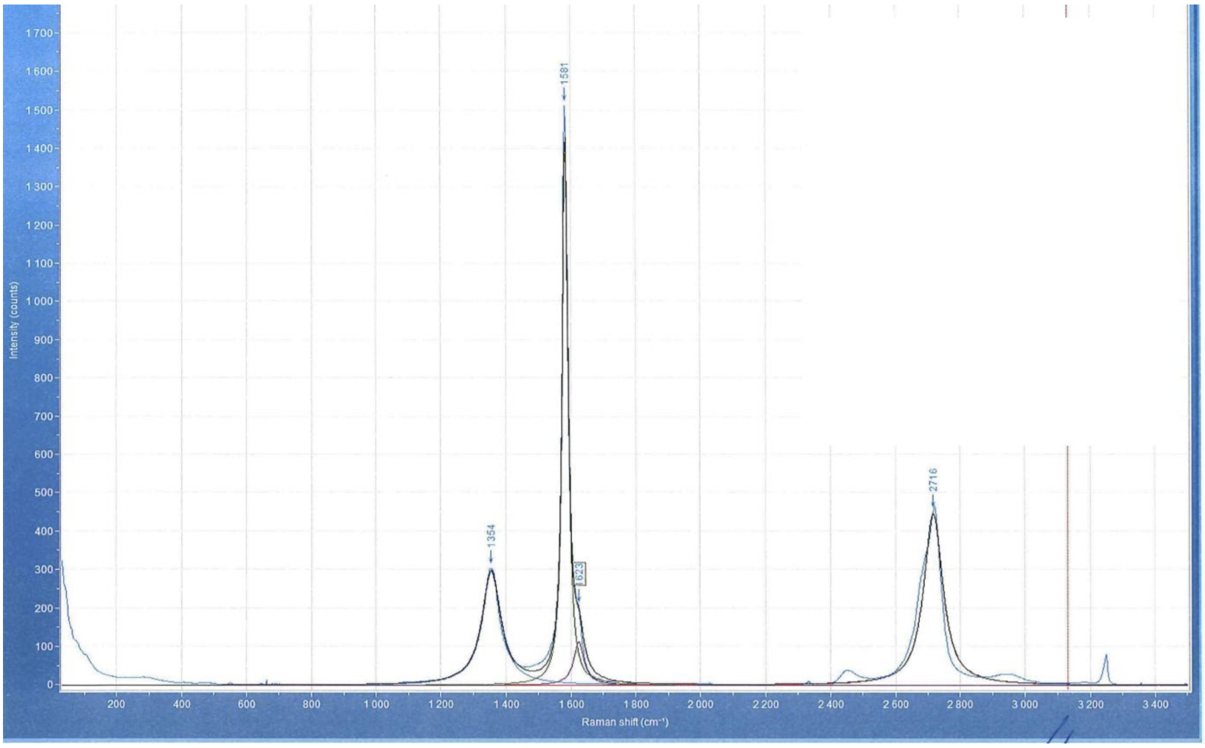


**Fig. S20**. Raman spectrum for 4_rGO. Note: annotations intended for in-house use have been removed. We emphasise that it is only the annotations that were removed, the spectra themselves have not been altered in any way.

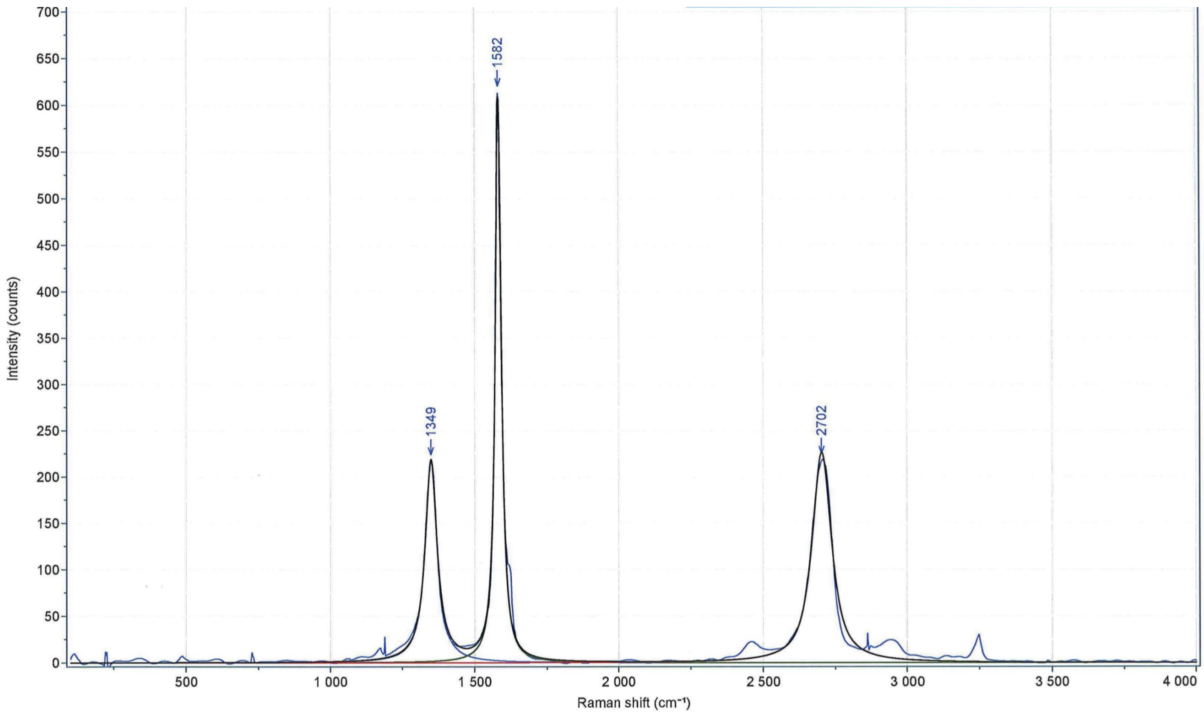


**Fig. S21**. Raman spectrum for 5_GNP

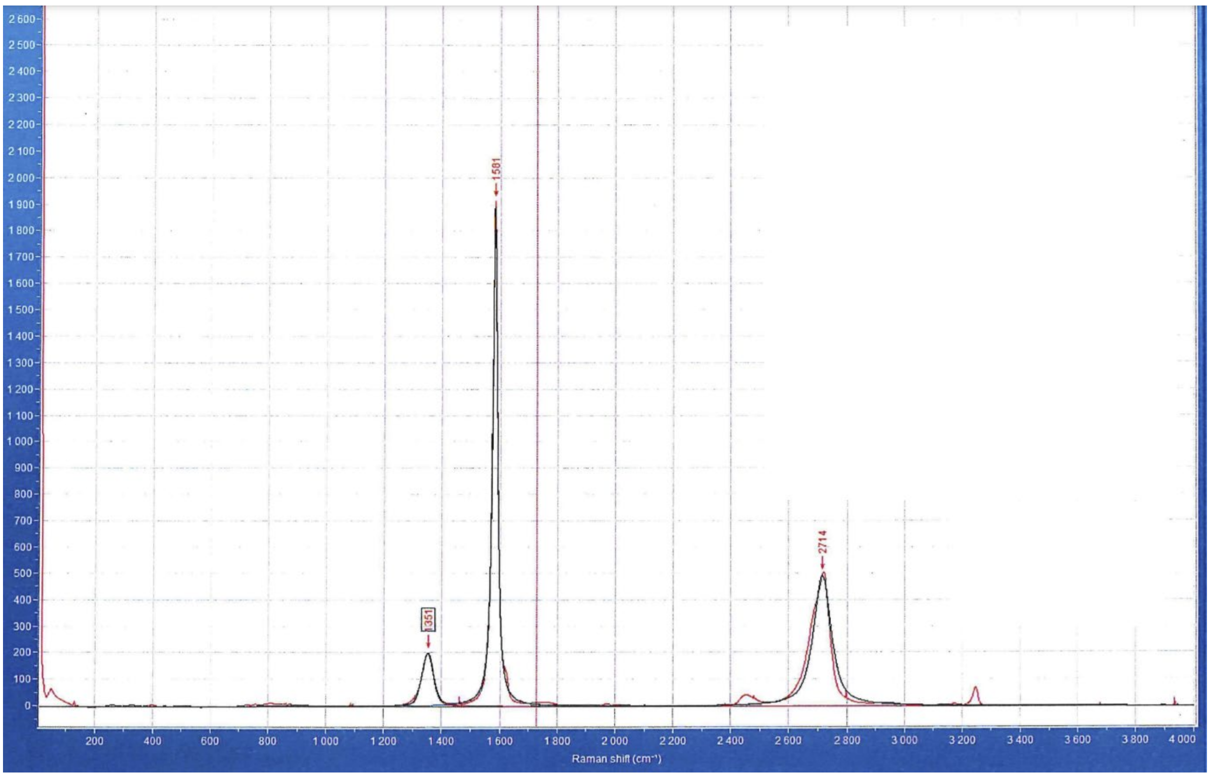


**Fig. S22**. Raman spectrum for 6_GNP. Note: annotations intended for in-house use have been removed. We emphasise that it is only the annotations that were removed, the spectra themselves have not been altered in any way.

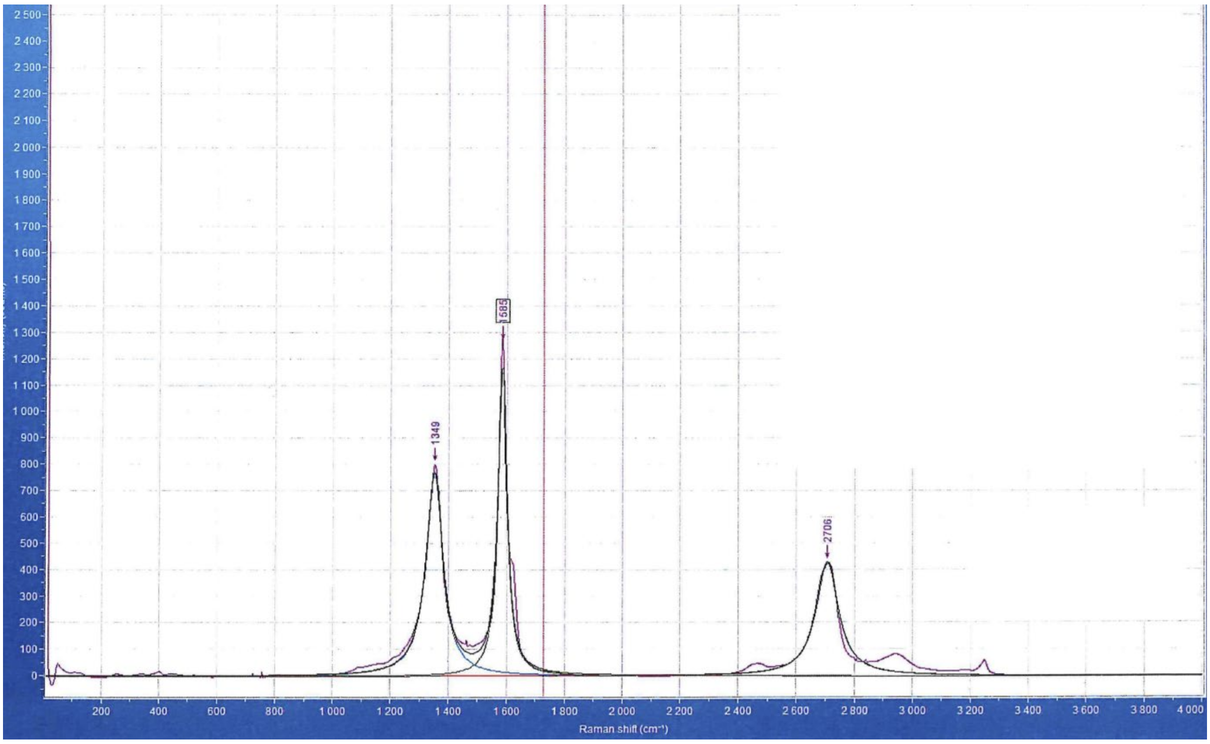


**Fig. S23**. Raman spectrum for 7_GO. Note: annotations intended for in-house use have been removed. We emphasise that it is only the annotations that were removed, the spectra themselves have not been altered in any way.

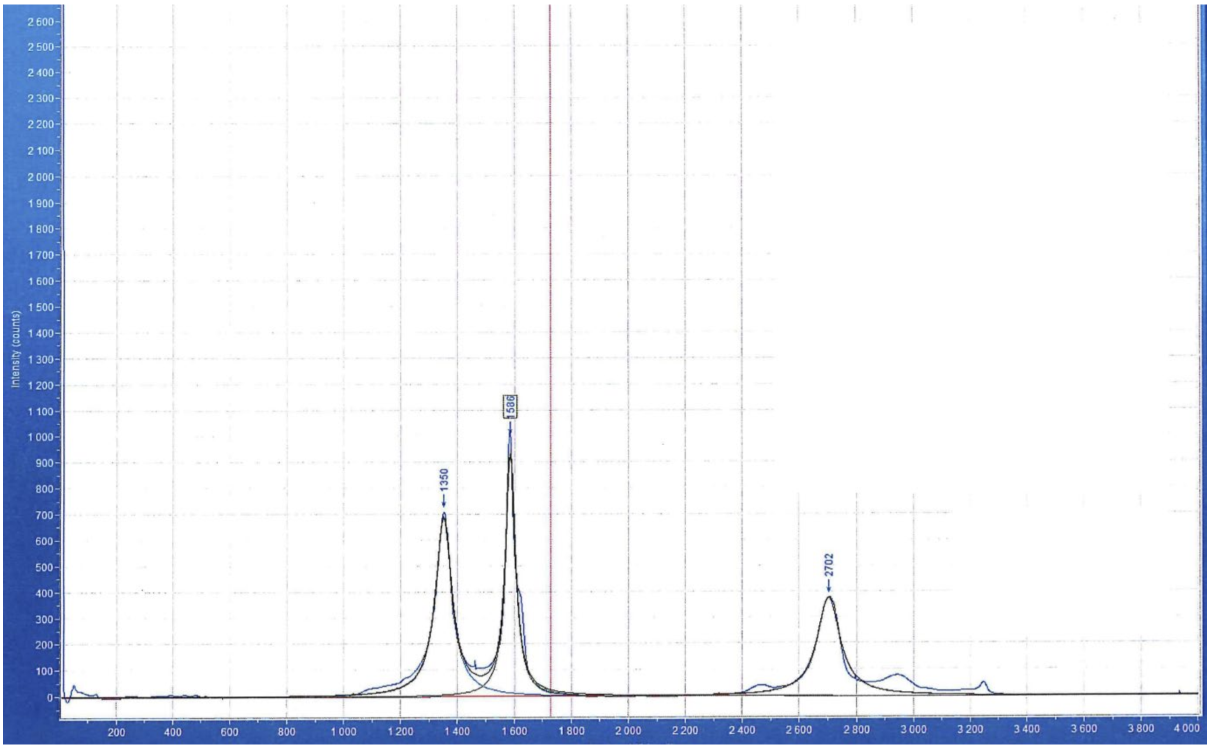


**Fig. S24**. Raman spectrum for 8_rGO. Note: annotations intended for in-house use have been removed. We emphasise that it is only the annotations that were removed, the spectra themselves have not been altered in any way.

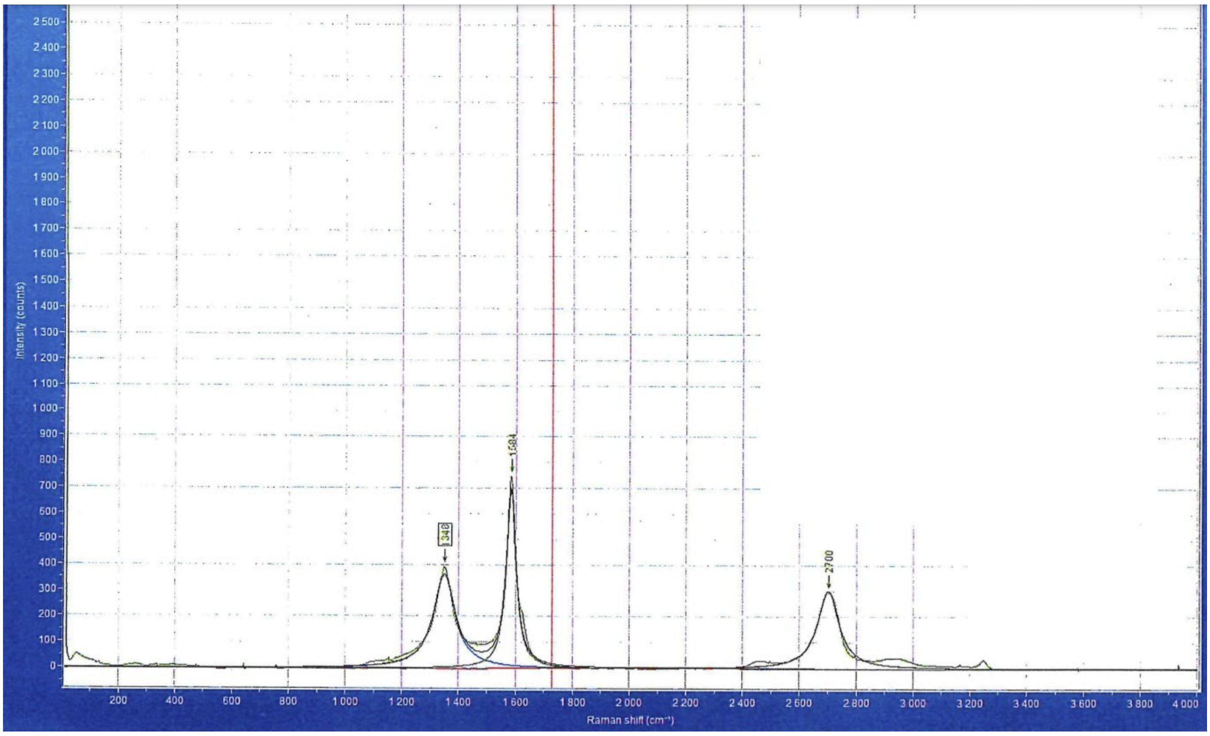


**Fig. S25**. Raman spectrum for 9_GNP. Note: annotations intended for in-house use have been removed. We emphasise that it is only the annotations that were removed, the spectra themselves have not been altered in any way.

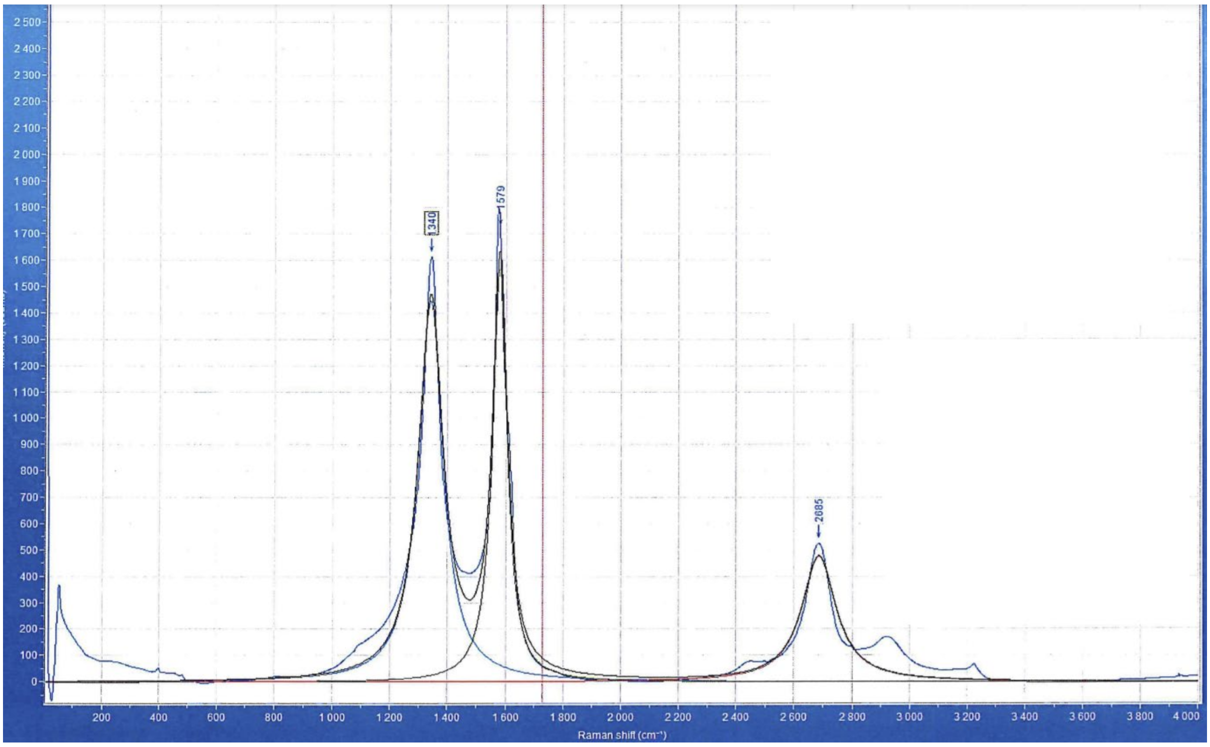


**Fig. S26**. Raman spectrum for 10_GO. Note: annotations intended for in-house use have been removed. We emphasise that it is only the annotations that were removed, the spectra themselves have not been altered in any way.

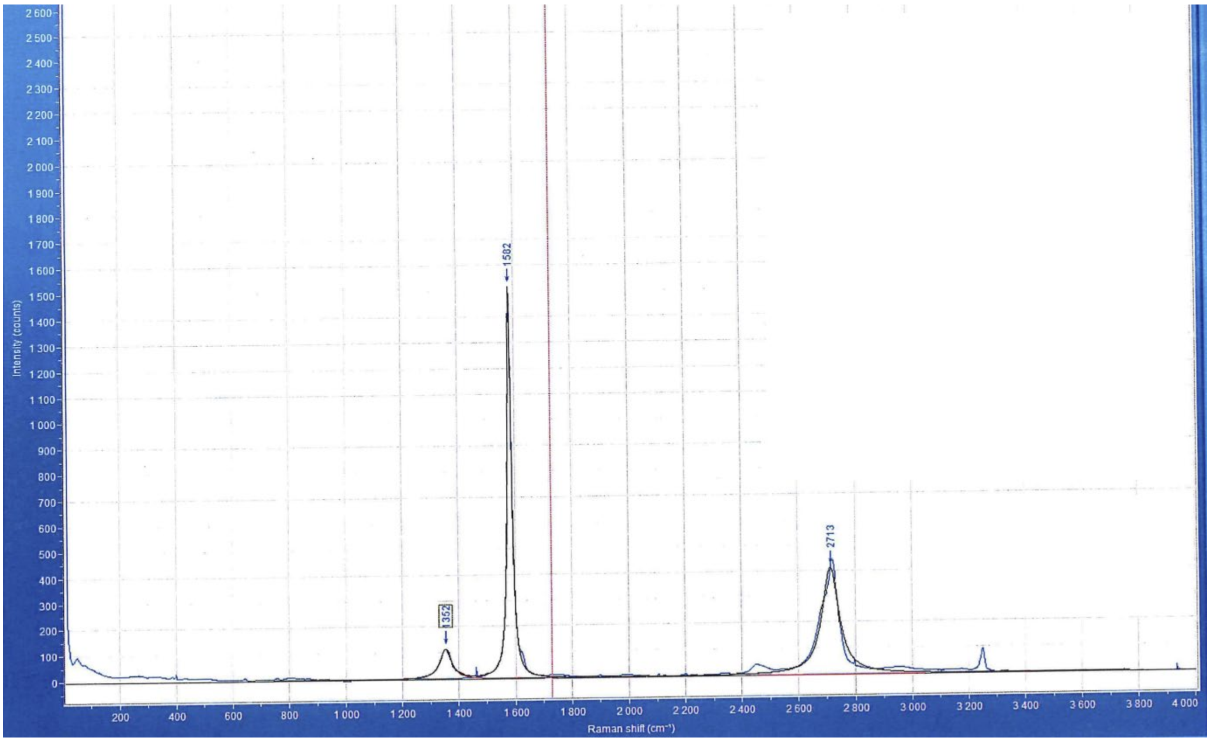


**Fig. S27**. Raman spectrum for 11_GNP. Note: annotations intended for in-house use have been removed. We emphasise that it is only the annotations that were removed, the spectra themselves have not been altered in any way.

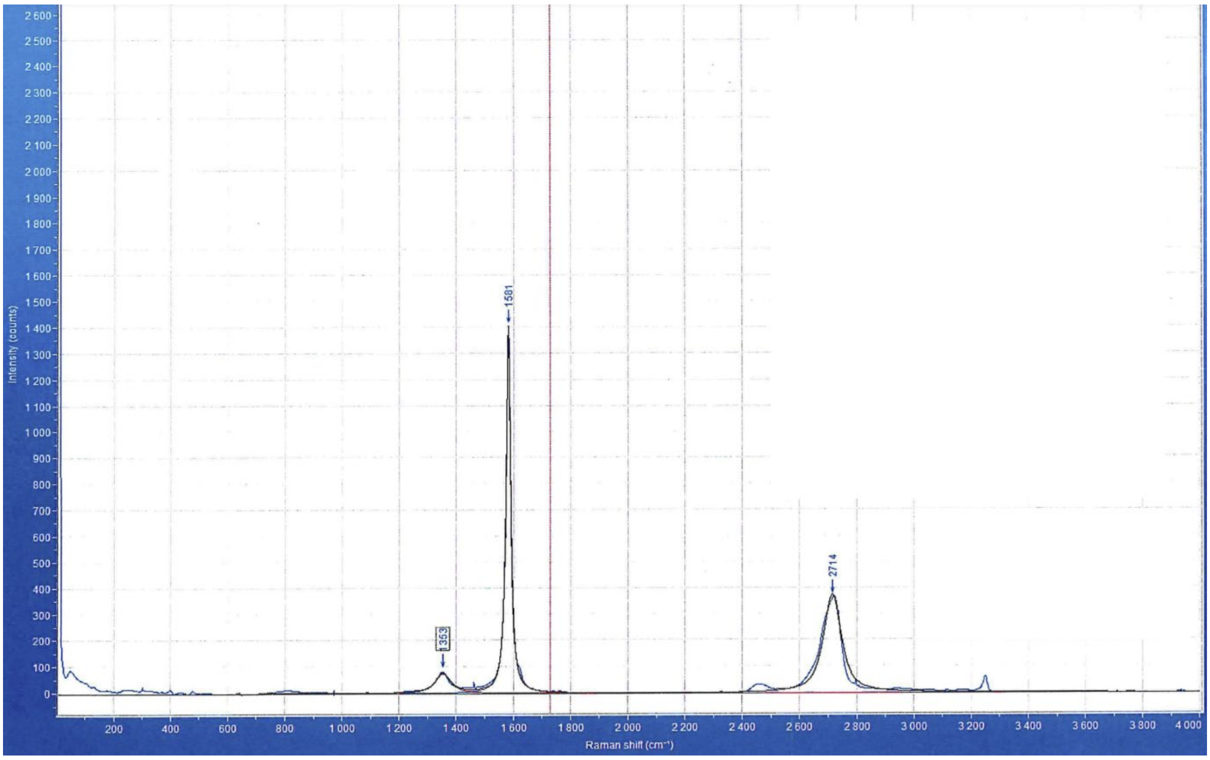


**Fig. S28**. Raman spectrum for 12_GNP. Note: annotations intended for in-house use have been removed. We emphasise that it is only the annotations that were removed, the spectra themselves have not been altered in any way.

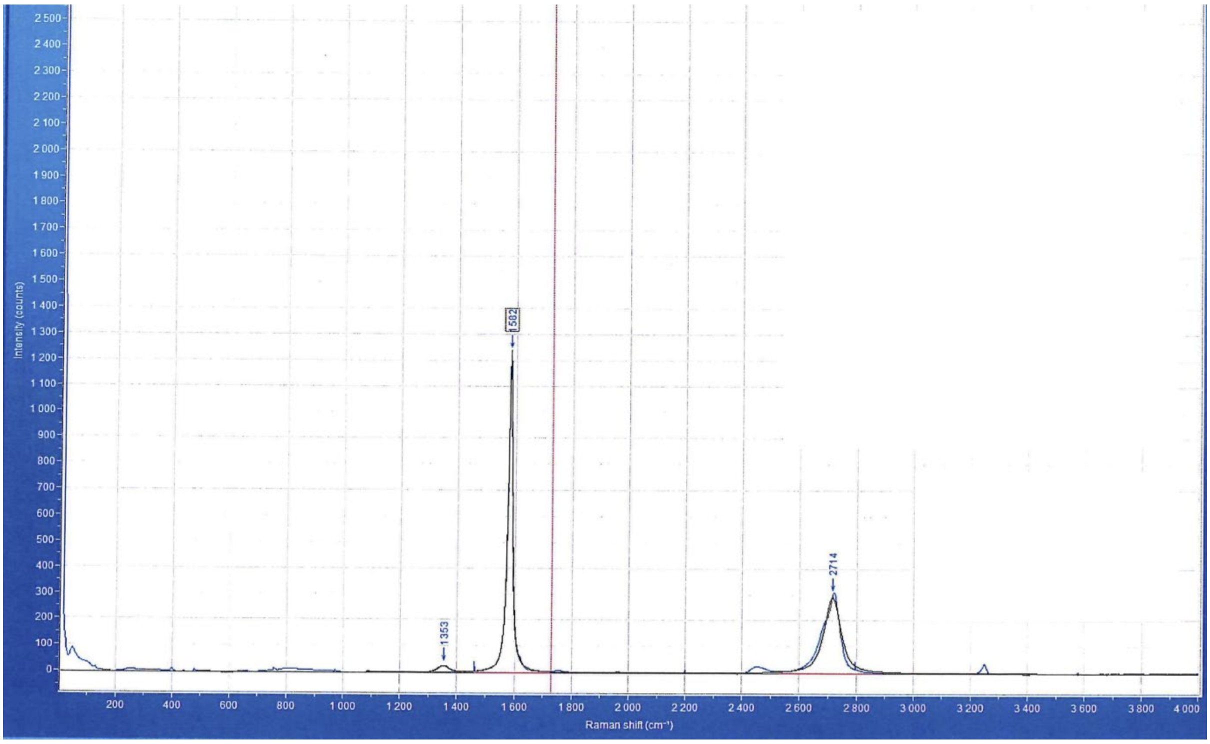


**Fig. S29**. Raman spectrum for 13_GNP. Note: annotations intended for in-house use have been removed. We emphasise that it is only the annotations that were removed, the spectra themselves have not been altered in any way.

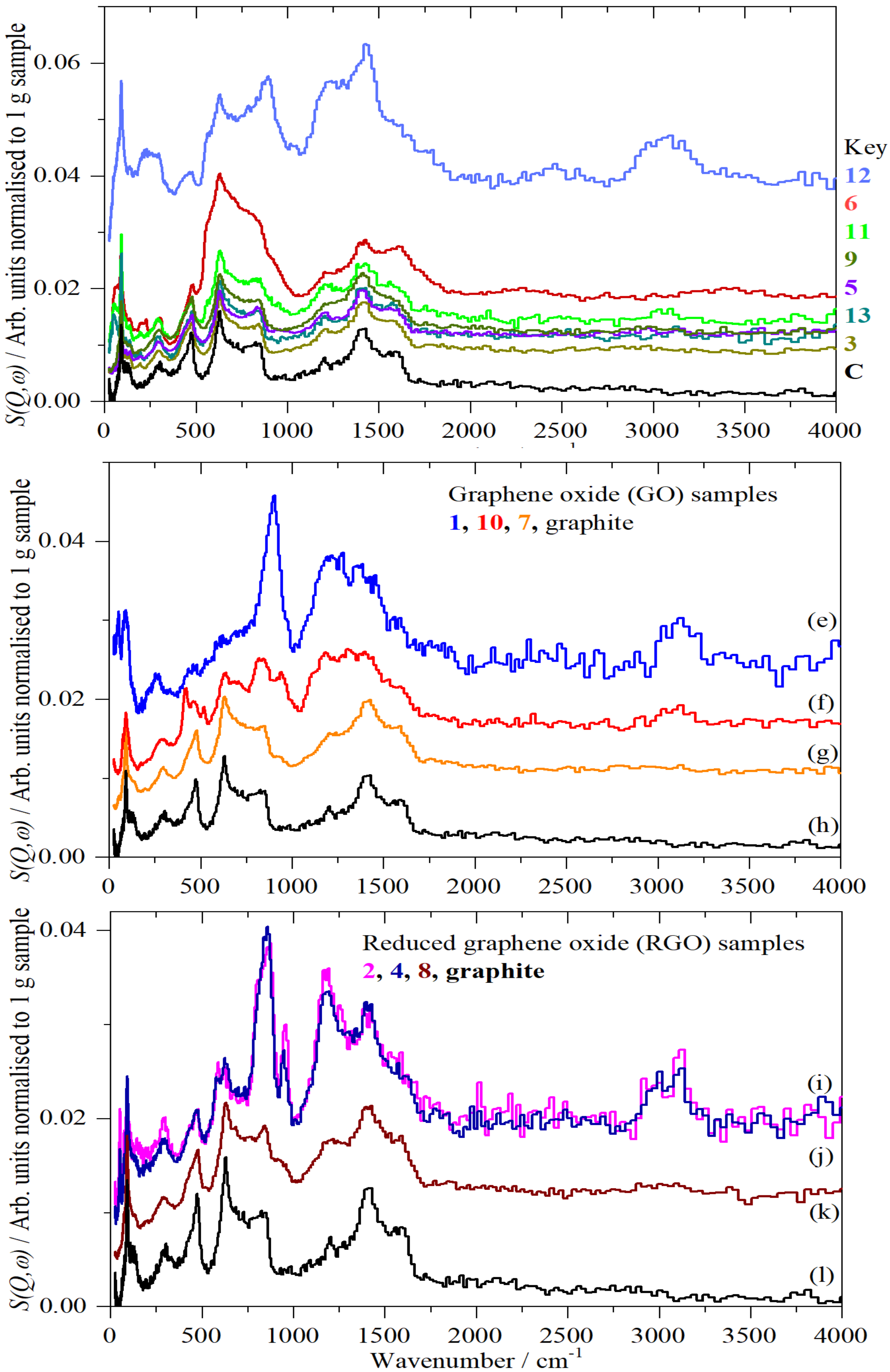


**Fig. S30.** Full range (0-4000 cm-1) TOSCA INS spectra of the 2D carbon samples. In each panel the bottom-most spectrum is a reference spectrum of graphite. Top panel: graphene samples. Middle panel: graphene oxide samples. Bottom panel: reduced graphene oxide samples.

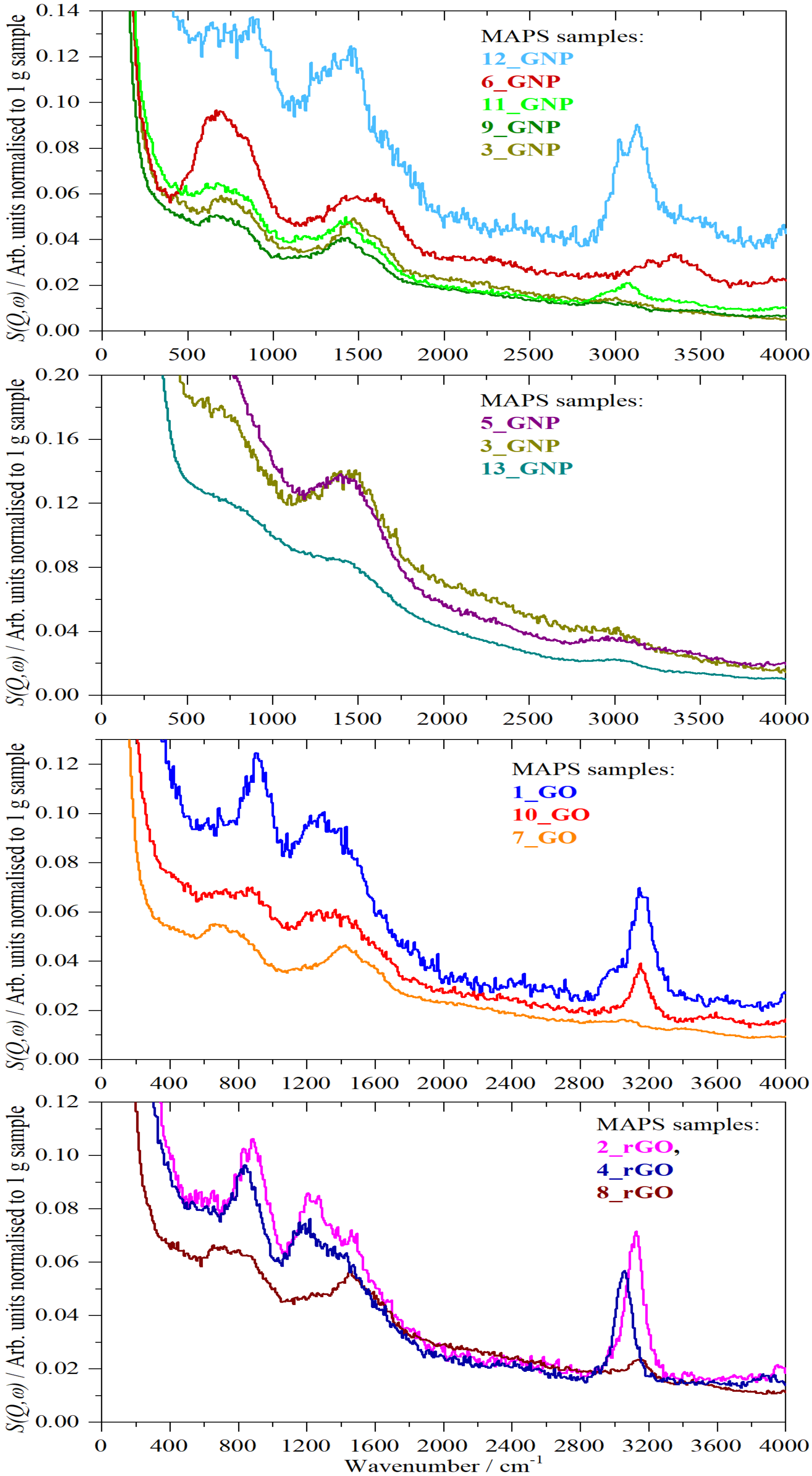


**Fig. S31.** MAPS INS spectra (0 – 4000 cm$^{-1}$) of the 2D carbon samples.

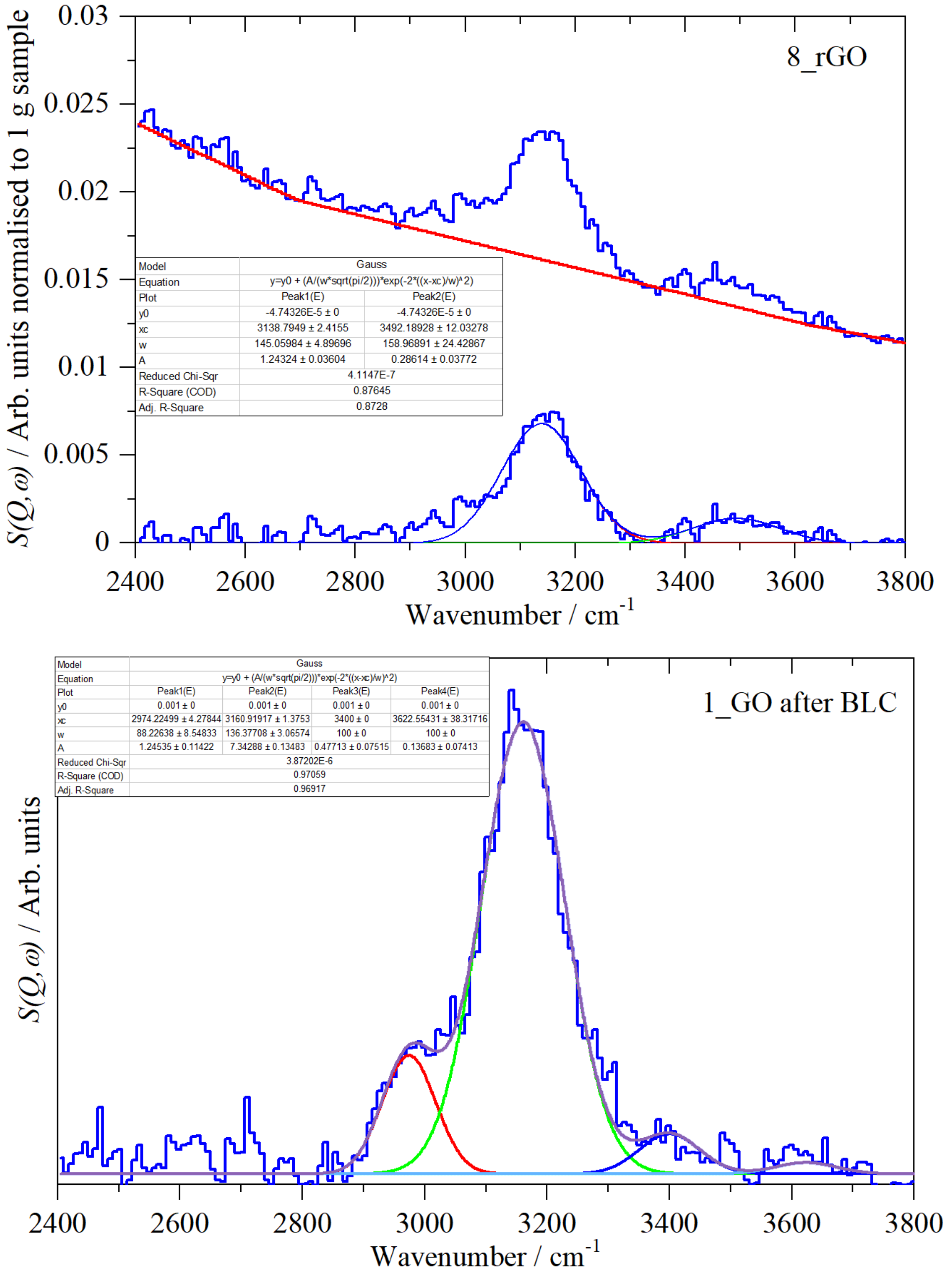


**Fig. S32.** Examples of curve fitting of the MAPS spectra in the C–H and O–H stretch region. The process first involves baseline correction (BLC) and then fitting to the minimum number of Gaussian functions. Top: 8_rGO, bottom: 1_GO.

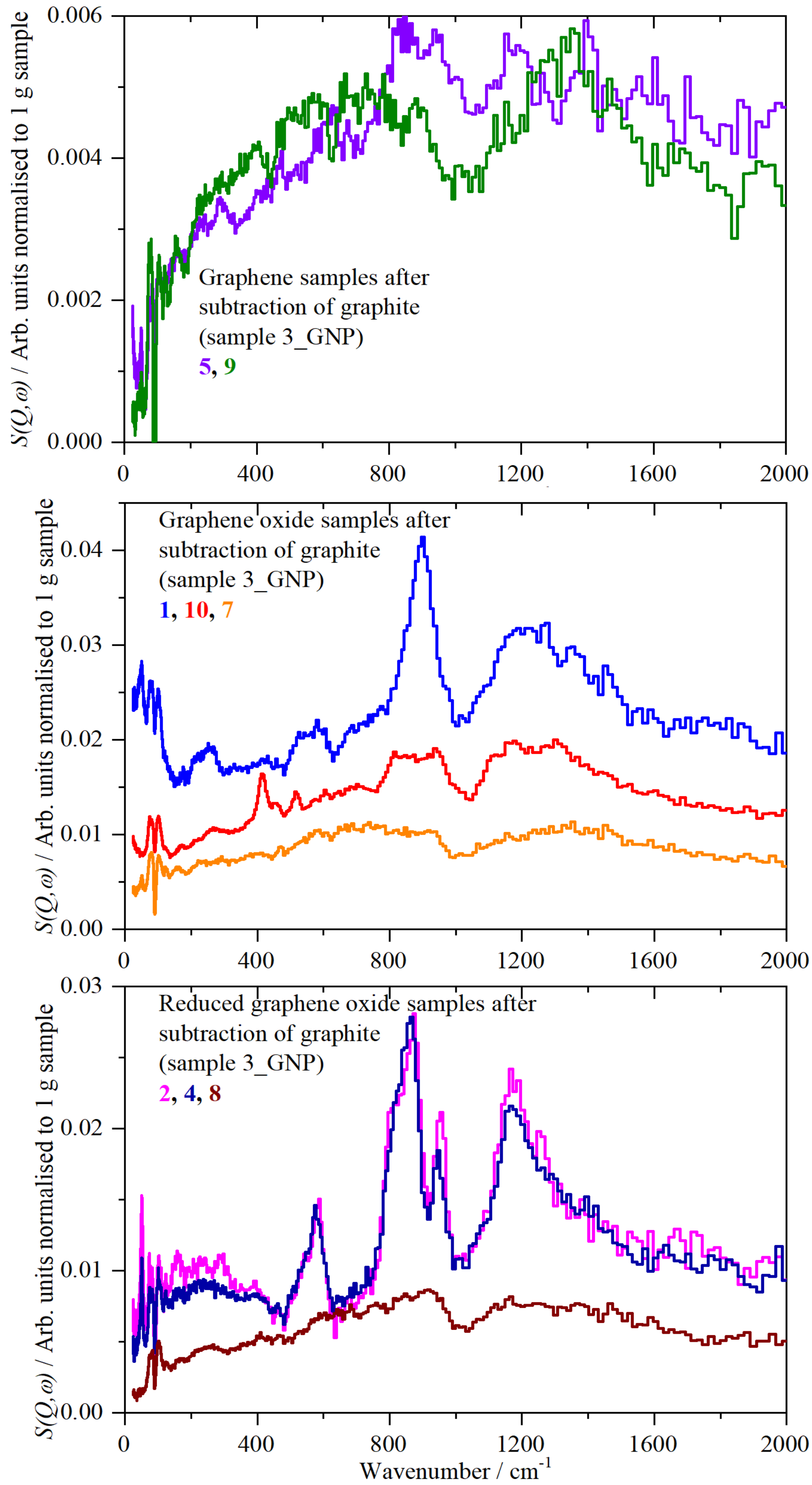


**Fig. S33.** TOSCA spectra of the 2D carbon samples after subtraction of the graphite contribution (3_GNP), grouped by sample type. Top panel graphenes: a) 5_GNP, b) 9_GNP. Middle panel graphene oxides: c) 1_GO, d) 10_GO, e) 7_GO (×2 ordinate expanded). Bottom panel reduced graphene oxides: f) 2_rGO, g) 4_rGO, h) 8_rGO. Note the different ordinate scales in the three panels.

**Table S3**

Correlation of 90 $cm^{-1}$ feature in the INS spectra with the width of the XRD peak at 26.5° (001).

| Sample | Half-width of $2\theta$ signal (ca. 26.5°) / Degrees | 90 $cm^{-1}$ peak width / $cm^{-1}$ |
|---|---|---|
| 1_GO | 4.85 | 29.5 |
| 2_rGO | 4.25 | 20.5 |
| 3_GNP | 0.749 | 9.1 |
| 4_rGO | 1.306 | 10 |
| 5_GNP | 0.381 | 9.1 |
| 6_GNP | 0.506 | 8.9 |
| 7_GO | 0.904 | 7.6 |
| 8_rGO | 0.925 | 7.6 |
| 9_GNP | 1.795 | 10.7 |
| 10_GO | 1.613 | 29.9 |
| 11_GNP | 0.582 | 8.1 |
| 12_GNP | 0.536 | 11.9 |
| 13_GNP | 0.658 | 8 |

**Explanation of the 12 $cm^{-1}$ feature in Fig. 12a.**

The intense peak at 12 $cm^{-1}$ observed in the simulated INS spectrum of graphene (Fig. 12a) does not originate in interlayer motion, unlike the 90 $cm^{-1}$ peak in graphite. The conversion from the phonon density of states (*G(ω)* which is what is calculated) to the experimentally observable *S(Q,ω)* involves multiplication by $1/\omega$ [2]. For a regular 3D material, the density of states of acoustic phonons at low energy roughly scales with frequency in a parabolic shape. This has the important implication that because the phonon DOS dies out faster than the $1/\omega$ term can boost the INS intensity as $\omega \rightarrow 0$, the overall INS intensity converges to zero. For 2D graphene, however, its phonon DOS near zero frequency converges to a finite value due to the quadratic flexural mode (and the fact that we now have a 2D reciprocal space). As a result, we lose an important counter-balance to the $1/\omega$ term and hence see the apparent divergence of intensity at low energy.

**References**

[1] P. Albers, A. Karl, J. Mathias, D. K. Ross, S. F. Parker, INS-, XPS- and SIMS-investigations on the controlled post-oxidation of pigment blacks – Detection of different species of strongly adsorbed water, *Carbon* 39 (2001) 1663-1676, https://doi.org/10.1016/S0008-6223(00)00294-3.

[2] G. L. Squires, *Introduction to Thermal Neutron Scattering*, Dover, 1996, pp54-56.